Energy & Buildings 357 (2026) 117179

Contents lists available at ScienceDirect

Energy & Buildings

journal homepage: www.elsevier.com/locate/enb

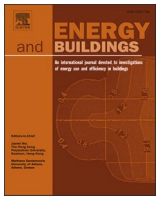

Data-driven characterization of start-up thermal response for optimal HVAC operation in tertiary buildings

M. García-Monge *, S. Guillén-Lambea, B. Zalba

Engineering Research Institute of Aragón (I3A), Thermal Engineering and Energy Systems Group (GITSE, University of Zaragoza, Agustín de Betancourt Building, C/ María de Luna 3, 50018 Zaragoza, Spain

ARTICLE INFO

Keywords:
Thermal response
Thermal inertia
Energy efficiency
HVAC control
Data-driven
IoT
Smart campus

ABSTRACT

This paper presents a methodology for analysing the thermal behaviour of tertiary buildings under intermittent heating schedules aligned with occupancy patterns. The approach aims to enable more efficient, dynamic HVAC operation based on a data-driven model. A central component of the methodology is the characterization of the coupled building-HVAC thermal response upon system activation, determined through a systematic analysis of start-up events from historical sensor data.

Validated across 62 buildings and almost 1,500 temperature sensors at the University of Zaragoza during the 2024–2025 heating season (October to April), the analysis revealed substantial variations in thermal response rates, varying tenfold from 0.3 to 3.0 °C/h. This heterogeneity confirms that the existing uniform, campus-wide HVAC schedule is suboptimal and demonstrates the necessity of personalized start-up strategies, according to the distinct thermal dynamics of each building.

The results have provided a clearer picture of the combined behaviour of the building, HVAC system, and climate, particularly during the preheating phase. The findings highlight the potential of this data-driven approach to support customized HVAC control strategies to ensure thermal comfort while reducing energy consumption. Crucially, this work addresses the implementation gap frequently reported in the literature, where sophisticated theoretical models remain incompatible with conventional building control systems. By prioritizing empirical validation over simulation, the proposed methodology offers a practical and readily deployable alternative to static, pre-defined control schedules that continue to dominate the existing building stock due to technological inertia.

1. Introduction

Buildings in the European Union account for approximately 40% of energy consumption, and an estimated 75% of the building stock is considered energy inefficient [1]. This inefficiency is largely due to the age of most buildings, constructed before the first energy efficiency regulations were introduced in 2002 [2]. Beyond the issue of energy inefficiency, inadequate building performance frequently gives rise to suboptimal thermal comfort and compromised indoor environmental quality.

The widely known hierarchy of actions for moving toward Zero Energy Buildings (ZEB) is established by the UNE-EN ISO 52000–1:2019 standard [3]. First, the reduction of energy demand through improvements in the building structure. This includes the quality of the building envelope (e.g. insulation, high-performance windows), the application of bioclimatic design strategies (such as daylighting), and the optimisation of thermal inertia and zoning. At this stage, it is also essential to guarantee proper indoor environmental conditions to prevent negative impacts such as poor indoor air quality due to insufficient ventilation or hygrothermal problems like mould growth. Second, the improvement of the energy efficiency of technical building systems, including heating, ventilation and air conditioning (HVAC), domestic hot water production, and lighting installations. Third, the integration of renewable energy sources, for example through active solar systems or district and collective heating and cooling networks that use renewable energy such as biomass, renewable gases, or waste heat recovered from industrial processes.

While this hierarchy provides a clear order of priorities, its practical implementation is often constrained by cost-effectiveness and feasibility. Deep renovations targeting the building envelope (Step 1), though

* Corresponding author.
E-mail address: miguelgmra@unizar.es (M. García-Monge).

https://doi.org/10.1016/j.enbuild.2026.117179
Received 3 December 2025; Received in revised form 1 February 2026; Accepted 15 February 2026
Available online 17 February 2026

essential for minimising energy demand, are typically costly and disruptive. In contrast, optimising the operation and control of technical building systems (Step 2) presents a more immediate and cost-effective pathway to enhance performance. In this context, Building Automation and Control Systems (BACS) play a fundamental role.

Historically, building energy efficiency strategies have often underestimated the contribution of automation. However, recent studies [4] and standardization efforts, notably ISO 52120–1:2021 [5], have demonstrated the significant energy savings achievable through BACS [6]. The integration of Internet of Things (IoT) technologies into BACS [7–9], including sensors, actuators, intelligent control algorithms [10,11], communication networks, and software platforms, further enhances this potential to optimize building performance.

This approach aligns with the concept of smart buildings as defined in the Energy Performance of Buildings Directive (EPBD) 2018/844/EU [12]. The same directive also introduced the Smart Readiness Indicator (SRI) [13]. The SRI evaluates a building's smart readiness based on its ability to perform three key functions: optimising energy efficiency and overall performance in use; adapting its operation to the needs of the occupant; and adapting to network signals (e.g. energy flexibility). The SRI thus informs building owners and managers about the automation and monitoring levels of their systems, aiming to encourage the adoption of smart technologies and serving as a guide for retrofitting actions [14].

Among technical building systems, Heating, Ventilation and Air Conditioning (HVAC) account for a substantial share of total energy use, often reaching up to half of the overall consumption [15,16]. Therefore, the effective management of these systems, including appropriate control of operating schedules, setpoints, ventilation rates, and equipment sequencing is essential to ensure satisfactory Indoor Environmental Quality (IEQ) while minimising energy demand, often with relatively low investment. The potential for advanced control spans a wide spectrum. In heat emission control, for instance, buildings can range from having no automatic room temperature control to implementing fully individual modulating control integrated with occupancy detection and BACS communication. Similarly, for flexibility and grid interaction, heating systems can progress from simple scheduled operation to fully optimized, predictive control that responds dynamically to performance forecasts and external grid signals. These examples illustrate the functionalities evaluated by the SRI, highlighting how intelligent automation improves energy efficiency, occupant responsiveness, and grid flexibility.

1.1. State of the Art: HVAC operation

Regarding HVAC schedules, Fadzli Haniff et al. [17] review various scheduling techniques for central HVAC systems. The most widely adopted conventional method, the "baseline approach", involves continuous HVAC operation. This strategy maintains a lower setpoint temperature for heating or a higher one for cooling during unoccupied periods, such as overnight [18]. While this prevents peak heating demands upon restart, it typically leads to higher energy consumption due to 24-hour operation. For this reason, a wide range of educational buildings, including universities, implement an occupancy-based HVAC control, which operate intermittently in accordance with occupancy schedules [19]. This involves a complete shutdown of HVAC systems during periods when the building is unoccupied. Consequently, in periods of unoccupancy (e.g. nights, weekends, or public holidays) during the heating season, both the building envelope and indoor air experience a cool-down process. Following a system restart, a specific duration is necessary for the indoor air temperature to return to its designated setpoint. This recovery or preheating period [20] ensures that desired thermal conditions are met before occupants arrive [21]. Sun et al. propose a new method to estimate the preheating time in intermittent heating with hot-water radiators, considering model uncertainties [22]. In subsequent work [23] they refine the approach to include variations in outdoor temperature and solar radiation, achieving over 80% accuracy in the model. Esrafilian-Najafabadi et al. [24] propose a novel RB control system that integrates a deep learning algorithm, specifically, a Multi-Layer Perceptron (MLP) network, to dynamically estimate the preconditioning time online. This approach uses historical data on outdoor weather, indoor temperature, and HVAC lag time to provide a more accurate estimation, aiming to improve energy savings without incurring the high complexity of Model Predictive Control (MPC).

Commonly, the preheating time required for intermittent HVAC operation during the heating season exhibits substantial variability across buildings. This variability is primarily governed by two parameters: the building's indoor air temperature at system start-up and the building's thermal response to HVAC activation, which determine the rate at which indoor air temperature increases. This is influenced by several factors, including the building's material properties, thermal inertia, outdoor conditions, and HVAC system characteristics. A building's overall thermal behaviour, as noted by Verbeke et al. [25], results from the complex interaction between heat gains, losses, and storage within its materials.

The phenomenon of heat transfer through the building envelope is driven by thermal gradients and pressure differentials. It is the thermal gradients that cause the transmission of heat via conduction through the envelope's materials, in combination with convective and radiative exchange at its surfaces. Pressure differentials drive advective heat transfer through bulk air movement, primarily infiltration via uncontrolled leakage pathways. The magnitude of these energy losses is contingent on the building's thermal insulation and airtightness, which in turn determines the required preheating duration. Consequently, a well-insulated, airtight building in winter will cool more slowly, thereby maintaining a higher internal temperature during off-cycles. This higher baseline, when combined with reduced ongoing heat loss, enables the heating system to reach the setpoint more quickly upon reactivation.

The thermal inertia of a building is a pivotal factor in determining its response to intermittent HVAC operation. Thermal inertia refers to the ability of building materials to store and release heat, thereby resisting and delaying fluctuations in indoor temperature caused by changes in outdoor conditions or internal heat sources [26,27]. This property is a function of the materials' thermophysical properties (i.e., mass, density, and specific heat capacity) and their strategic placement, such as the relative position of mass and insulation [28]. In the context of high-mass buildings, the HVAC system is required to condition not only the indoor air volume but also the building structure itself. This additional requirement results in a gradual temperature rise, thereby extending the preheating period and potentially necessitating greater HVAC system capacity to manage the total thermal load [25].

In HVAC system design, the ratio of available power (system capacity) to thermal demand is a critical parameter. An undersized system may fail to reach the temperature setpoint in a timely manner, thus extending the preheating period. The building's thermal response is also heavily dependent on the heating emitters. As noted by Karlsson et al. [29], different heating systems exhibit varying levels of thermal inertia based on their design and configuration. For instance, radiant floor systems are characterized by substantially higher thermal inertia than fan coil units, leading to a slower thermal response. Furthermore, in hydronic systems, the rate of heat delivery is directly governed by the supply water temperature. Consequently, Chen et al. [30] propose a control strategy involving an initial high-temperature supply, which is subsequently reduced once a steady-state condition is achieved. Karlsson et al. [29] also underscore the significance of incorporating the lag time into the assessment. The term "lag time" refers to the purging time or the transport time required for the water to traverse the heating system.

Therefore, the synergistic effect between the building's and the HVAC system's thermal inertia exerts a combined and decisive influence on the thermal response of indoor air [31]. This synergy indicates that even buildings with substantial thermal mass can achieve shorter

recovery times if the HVAC system is capable of effectively compensating for the building's thermal characteristics.

In the field of thermal inertia, the majority of authors have opted for theoretical modelling and simulations as a primary research method, rather than relying on experimental studies [32]. This approach is primarily influenced by the inherent challenge of isolating the impact of thermal inertial phenomena from other influencing factors, such as local climatic conditions and occupant behaviour [25]. For instance, to characterise the thermal inertia of a building, authors such as Orosa et al. [33], calculate its time constant determined by analysing the decay rate of the indoor temperature during a simulated slow cool-down period with a constant low outdoor temperature. The time constant is a key metric used to quantify a building's thermal inertia, which expresses the ratio of the building's total heat capacity to its overall heat loss factor.

However, relying exclusively on such theoretical simplifications can lead to significant discrepancies when applied to operational infrastructure. As Herrando et al. [34] demonstrated in their analysis of faculty buildings in Spain, a substantial divergence frequently exists between simulated energy ratings and actual consumption, a phenomenon widely recognized as the "building energy performance gap". This gap arises because theoretical models often require simplifying hypotheses that fail to capture the stochastic nature of real-world variables. For instance, while simulations assume ideal conditions, Uriarte et al. [35] highlight the experimental complexity of decoupling specific physical parameters, such as transmission and infiltration heat loss coefficients, in in-use office buildings. These studies suggest that the rigid assumptions of pure physical modelling may not sufficiently account for the multitude of uncertainty sources inherent in large-scale, existing building stocks.

A key application of thermal inertia research is in enhancing the energy flexibility of buildings, particularly through the management of thermostatic loads from HVAC systems [36,37]. Building flexibility is defined as the ability of buildings to alter their demand or generation depending on weather conditions, user needs and grid requirements [38]. In this context, a building's thermal mass can be leveraged as an inherent thermal energy storage medium. This storage capability allows control strategies to shift HVAC energy consumption by controlling the temperature of the HVAC system area without compromising occupant's comfort [36]. This effectively alters the building's demand profile to better align with grid requirements. Huang et al. [37] experimentally characterized the integrated thermal response of five buildings, a metric combining the inertia of both the building and its HVAC system. Their method involved analysing operational data from thermostat excitation signals and implementing a zone setpoint temperature change of 1°C. Their results, derived from cooling experiments, showed normalized response times of 1 to 5 hr/°C, equivalent to a rate of change of 0.2 to 1.0 °C/h.

1.2. Research gaps and proposal

Despite the extensive literature on adaptive preheating, two critical gaps remain in the state of the art:

1. **The scarcity of large-scale experimental validation**. As highlighted by Verbeke et al. [25], "instead of measurement campaigns, most authors have opted for theoretical models and simulations", with only a few comparative monitoring campaigns reported. Theoretical models often rely on simplifying hypotheses that fail to capture the stochastic nature of real-world variables. Therefore, there is a pressing need for research based on empirical data measured in operational buildings rather than simulated environments. Previous studies such as Huang et al. [37] use measured data from buildings, but on a limited time scale and number of buildings.
2. **The lack of deployable solutions for existing infrastructure** (implementation gap). Even among studies utilizing real data, the proposed algorithms typically present significant barriers to large-scale implementation:
   - Grey/White-box limitations: Works such as Sun et al. [22] rely on detailed physical parameters often unavailable or uncertain in existing buildings [25], or requires labor-intensive calibration for each specific thermal zone, severely limiting its scalability beyond pilot rooms.
   - Computational barriers: Similarly, while Esrafilian-Najafabadi et al. [24] review sophisticated MPC strategies, these typically entail high computational demands and complex system identification processes.

This creates an implementation gap: sophisticated models exist, but they are incompatible with the standard Programmable Logic Controllers (PLCs) that manage the vast majority of the aging building stock.

The aim of this study is not to pursue the marginal accuracy gains associated with complex theoretical models, but rather to demonstrate how continuous monitoring can drive tangible performance improvements in HVAC systems, specifically during the critical start-up phase, at a large scale. Crucially, the proposed methodology is designed to be deployed using available technologies (standard PLCs), offering a viable and immediate alternative to the inefficient pre-set fixed schedules that still dominate the management of the aging building stock due to technological inertia.

Table 1 summarizes the comparison between previous studies and the approach proposed in this work.

To bridge these gaps, this study proposes a methodology for analysing the thermal behaviour of tertiary buildings operating under intermittent heating schedules aligned with occupancy patterns. The primary objective is to derive adaptive HVAC control strategies tailored to the specific thermal dynamics of each building enhancing both energy efficiency and occupants' thermal comfort.

A key component of this proposal is the characterisation of the building's thermal response solely during the preheating phase. The magnitude of this response is quantified through the rate of indoor temperature increase (°C/h), derived from continuous indoor temperature monitoring. A major advantage of this data-driven approach is that it does not require prior knowledge of the building's physical parameters. Instead, the complex interactions between building physics, indoor and outdoor conditions, and HVAC system performance are implicitly captured within the observed temperature data during these transient periods.

The resulting characterisation provides a robust, data-driven foundation not only for developing more efficient HVAC operational schedules but also for assessing the actual thermal performance of the facilities. Although the framework is broadly applicable to various types of tertiary buildings, this paper focuses on its application within university facilities, using the campuses of the University of Zaragoza (UNIZAR) as a case study. The goal is to improve energy management while addressing the critical implementation gap between theoretical potential and operational reality, demonstrating how scalable, data-driven logic can be deployed into conventional control systems to overcome the technological inertia of static scheduling.

2. Materials and methods

2.1. Materials

The present study focuses on the buildings of the University of Zaragoza (UNIZAR), a higher education institution, comprising six university campuses strategically located in the autonomous community of Aragón in Spain.

The "Campus FIDigital" project at UNIZAR constitutes an integrated ecosystem designed to facilitate data-driven decision-making for the efficient and sustainable management of university resources. This system is based on a "measure-analyse-decide-act" methodology,

Table 1
Comparison between previous studies and the approach proposed in this work.

Feature	Prior studies	This work
Primary Focus	**Temperature Prediction & Parameter Estimation.** Focuses on minimizing the error between predicted and measured temperatures or identifying physical properties. This objective requires modelling the complex thermal profile, forcing the inclusion of unpredictable variables like solar gain and occupancy variations to achieve accuracy.	**Start-up Isolation.** Targets the preheating phase (winter mornings), eliminating stochastic loads (lighting, occupancy, solar). By staying below steady-state saturation, the system operates in its linear response region, allowing a precise quantification of the heating slope (°C/h).
Nature of the study	White-box models: **Theoretical**. Primarily simulations (EnergyPlus, TRNSYS). Simplifying hypotheses combined with uncertain inputs lead to significant error propagation and fail to capture real-world stochasticity (Verbeke et al. [25]). Grey-box models: **Hybrid**. Combines physics with data but typically limited to controlled pilot experiments in a single room/building (Sun et al. [22,23]) or short-term calibration. Black-box models: **Algorithmic (opaque)**. Prioritizes statistical fitting over physical dynamics. Prone to overfitting and poor extrapolation outside the training domain. The resulting lack of interpretability hinders diagnosis and limits operator trust.	**Empirical** / Experimental. Based on real-world operational data (IoT/SCADA) of existing infrastructure. Captures the actual thermal response of buildings (unlike simulations) while providing physically interpretable metrics (unlike black-box models).
Scale of analysis and validation	Generally **unitary:** One building or one thermal zone.	**District** / campus **scale**: 62 buildings of a heterogeneous nature (different construction dates, insulation, HVAC systems, etc.). High number of sensors (~1,500). ~62,000 preheating periods analysed
Monitoring Campaign	**Short-term**. Often limited to a few days/weeks of validation or theoretical "typical meteorological year" simulations.	**Full heating season**: Continuous analysis from October to April (monitoring remains active).
Integration readiness	**Low** (requires external processing units/cloud) due to high complexity (differential equations, neural networks) and real-time data from a multitude of variables.	**High**, directly programmable into standard PLCs due to lower complexity (linear slope characterisation) and internal temperature.
Scalability	White-box models: **Low**. High modelling effort; requires defining complex geometry and physics for every individual building. Grey-box models: **Limited**. Requires iterative parameter identification (R-C values) by calibration for each specific thermal zone. In previous studies such as Sun et al. (2024) [23], the methodology only applies to low thermal inertia buildings. Black-box models: **Limited**. Training individual Neural Networks for each zone creates a massive computational and management overhead.	**High.** Offers an optimal trade-off: the linear characterization is computationally lightweight for large-scale implementation yet sufficiently accurate, as it specifically targets the linear heating segment of the start-up phase. The methodology works for any type of building, regardless of its inertia. Eliminates the need for individual model training, expert supervision, or complex parameter identification across hundreds of zones.
Data requirement	White/Grey-box models: **Heavy / High Uncertainty.** Requires weather forecasts and detailed physical parameters (R, C) often unavailable or uncertain in existing buildings (Verbeke et al. [25]). Black-box models: **High Volume / Intensive** Demands large, high-quality historical datasets for training.	**Minimal**. Relies exclusively on historical internal temperature logs (BMS or IoT ecosystem). Eliminates the dependency on external weather forecasts, solar radiation sensors, or geometrical/physical parameters that are difficult to obtain in existing buildings.

achieved by hybridizing physical elements with digital technologies. This integration leverages Building Management Systems (BMS), IoT platforms, and institutional information and metadata sources. The infrastructure incorporates a real-time monitoring system to collect data on critical parameters, including indoor environmental quality, occupancy patterns, and energy consumption. All collected data and associated campus elements are systematically integrated and georeferenced through a Spatial Data Infrastructure (SDI), which provides a spatially codified inventory of all university spaces and assets accessible via an integrated visualization platform, thereby enabling robust spatio-temporal analysis and informed management actions.

The data acquisition infrastructure implemented at the university is a hybrid architecture designed to integrate heterogeneous data streams from two distinct complementary subsystems: a wireless LoRaWAN (Long Range Wide Area Network) sensor network [39] and the wired Supervisory Control and Data Acquisition (SCADA). Both data sources converge at a centralized MQTT (Message Queuing Telemetry Transport) broker, which feeds a unified IoT platform for data processing.

The wireless subsystem is a low-power, wide-area network (LPWAN) based on the LoRaWAN specification, intended to address fundamental IoT requirements, including low energy consumption, long-range communication, end-to-end security, high interoperability, minimal maintenance requirements and cost-effectiveness. It is primarily deployed for localized monitoring, capturing parameters such as indoor environmental conditions, occupancy patterns, and specific end-use gas or electricity consumption. The data telemetry path for this subsystem originates at the end-devices, which transmit encrypted payloads. These transmissions are received by on-premises gateways and forwarded to The Things Network (TTN), which serves as the LoRaWAN Network Server (LNS) for packet deduplication, decryption, and management. Following validation, TTN integration forwards the application-level data by publishing it as an MQTT message to a centralized MQTT broker (EMQX).

Concurrently, the facility's existing SCADA system provides a high-reliability data stream from its wired instrumentation. This wired subsystem monitors core building services and central plant utilities, providing data not captured by the wireless network. Its scope includes main electrical and gas consumption, HVAC operational parameters (e.g., supply and return temperatures), wired indoor temperature readings, sanitary hot water (SHW) temperatures, and the operational status of equipment (e.g., boilers, pumps, and lighting circuits). In this subsystem, wired sensors and probes are directly interfaced with

Programmable Logic Controllers (PLCs). These PLCs communicate their data to the central, cloud-based SCADA system. This SCADA system, in turn, functions as the MQTT client, publishing the aggregated telemetry data stream to the same central EMQX broker utilized by the LoRaWAN subsystem.

The Thingsboard IoT platform is configured as a subscriber to the relevant MQTT topics on the EMQX broker. This platform handles the seamless ingestion, persistence, and analysis of the aggregated, complementary data streams. Critically, as data is ingested, it is assigned the specific spatial code of the monitored element within the building.

As for environmental conditions the "Campus FIDigital" project employs a multi-sensor approach that enables practical experimentation with a diverse range of environmental sensors sourced from different manufacturers, allowing comparative evaluation of sensor performance, accuracy, and interoperability. As summarized in Table 2., the wireless system integrates real-time monitoring of key indoor environmental parameters. These include carbon dioxide (CO_2) concentration, temperature, relative humidity, atmospheric pressure, light intensity, and indicators of indoor air quality.

With respect to the indoor temperature, there are at present close to 1500 sensors distributed across a total of 62 buildings, including both wired and wireless probes. Since all these sensors are wall-mounted, the analysis of the difference between operative temperature and indoor air temperature is performed under conditions favourable for comfort assessment; the sensor's direct contact with the wall typically results in measured values slightly lower than the room's ambient air temperature in heating mode. However, this discrepancy between operative and air temperature can be effectively adjusted by modifying the setpoint temperature. For instance, Fig. 1 presents a QGIS-generated (Quantum Geographic Information System) visualization of the Faculty of Philosophy and Arts, a recently refurbished building equipped with comprehensive temperature monitoring in all rooms. The figure effectively functions as a spatial heat map, depicting the distribution of indoor thermal conditions throughout the facility. As indicated by the legend, the colour symbology applied to each room corresponds to distinct intervals of interior temperature, which are further classified according to the operational heating mode.

The collation of all this data facilitates the analysis of building and HVAC systems behaviour. In short, the buildings of UNIZAR themselves constitute a large research laboratory.

2.2. Methods

The University of Zaragoza's building portfolio is highly heterogeneous, with a mean construction date of 1984 (Fig. 2). This variability, combined with subsequent renovations, has resulted in a diverse range of HVAC systems. These systems differ significantly in their central generation technology (ranging from traditional boilers to modern heat pumps), terminal units (such as radiators, fan coils, or radiant floors), air distribution methods, and the presence of mechanical ventilation, as well as their overall distribution designs and control capabilities. In this latter regard, older facilities, which often utilize ring or column systems, have limited zoning based typically on orientation (north-south). In contrast, newer constructions feature more complex circuits enabling more refined zoning by functional use (classrooms versus offices) and, in some cases, individual room control.

This section presents the methodology for developing and evaluating a data-driven HVAC scheduling model, moving from a generalized baseline to building-specific control. Buildings at the University of Zaragoza are typically occupied from 8:00 a.m. to 8:00 p.m., requiring HVAC systems to operate intermittently, activating before occupancy and deactivating at night. Up until this point, the activation times prior to occupancy have been based on 24-48-hour weather forecasts and applied uniformly across all buildings. This was due to the lack of real-time indoor monitoring and limited knowledge of individual building thermal dynamics.

Given the recently deployed monitoring system with almost 1500 sensors distributed across a total of 62 buildings, this study evaluates the feasibility of building- and zone-specific HVAC control strategies adapted to their unique thermal behaviour. The primary goal is to determine the optimal pre-conditioning time required for each zone to achieve the target comfort temperature at the start of occupancy. To determine this, thermal behaviour is characterized by analysing continuous indoor temperature data, specifically calculating the thermal response rate (the rate of temperature increase (°C/h) following HVAC activation). Unlike traditional approaches, this method leverages the transient behaviour of the building during daily operation, turning the routine cycling of the HVAC system into a valuable source of information. This approach not only facilitates the scaling of the analysis to a large number of buildings but also ensures that the results reflect the actual, in-use performance of the facilities

To automate this analysis, a Python program is developed to calculate the indoor temperature rise slopes (°C/h) during the initial heating system start-up. Fig. 3 illustrates this process for a single day, showing

Table 2
Sensors installed at University of Zaragoza (● = included measurement).

Sensors	Image	Temperature	Relative Humidity	CO_2	Atmospheric Pressure	Light Level	Presence	TVOC	Other Pollutants
Milesight EM300-TH		●	●						
Milesight AM307		●	●	●	●	●	●	●	
Aranet 4 Pro		●	●	●	●				
inBiot (Mica, Plus, Well)		●	●	●				●	●
Elsys ETHd10		●	●						

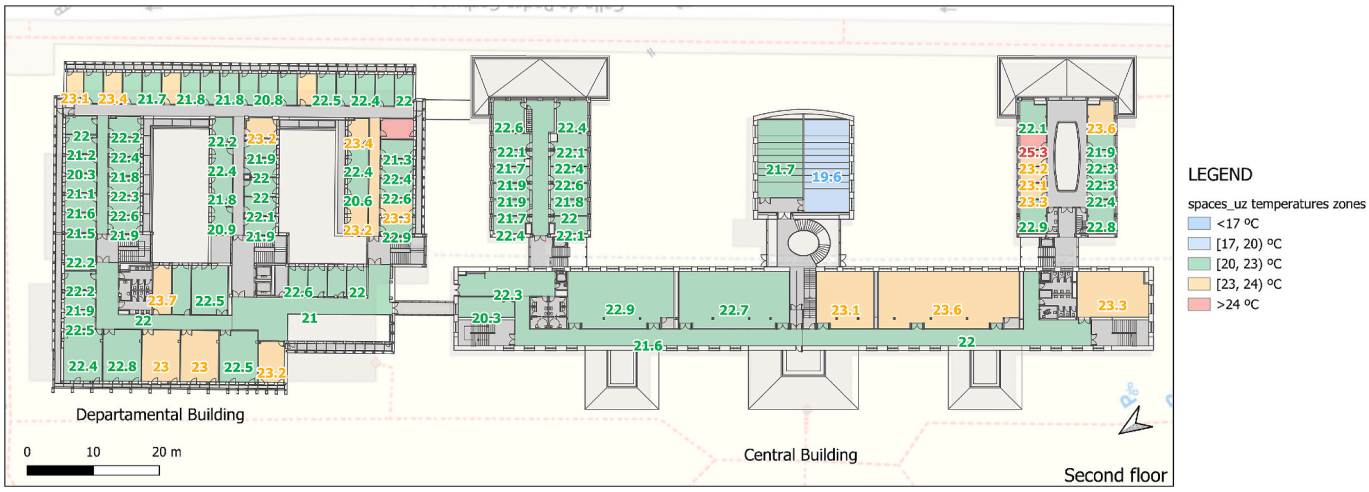

Fig. 1. Example of indoor temperature representation in buildings at the University of Zaragoza (QGIS).

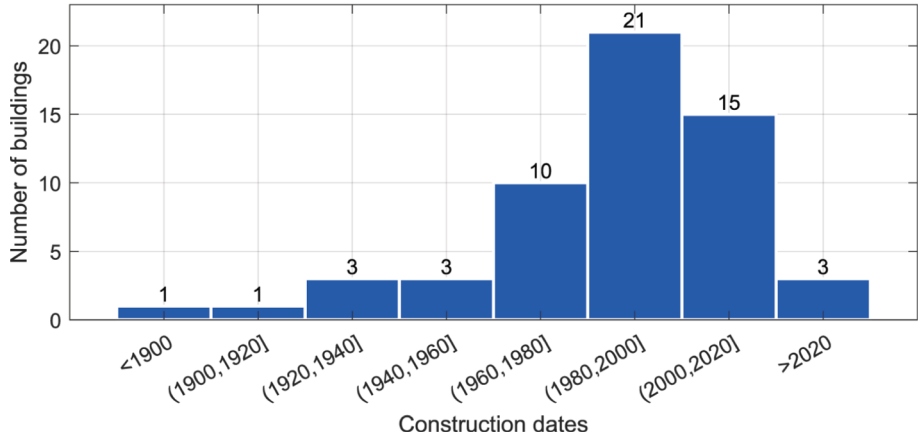

Fig. 2. Distribution of construction dates for buildings at the University of Zaragoza.

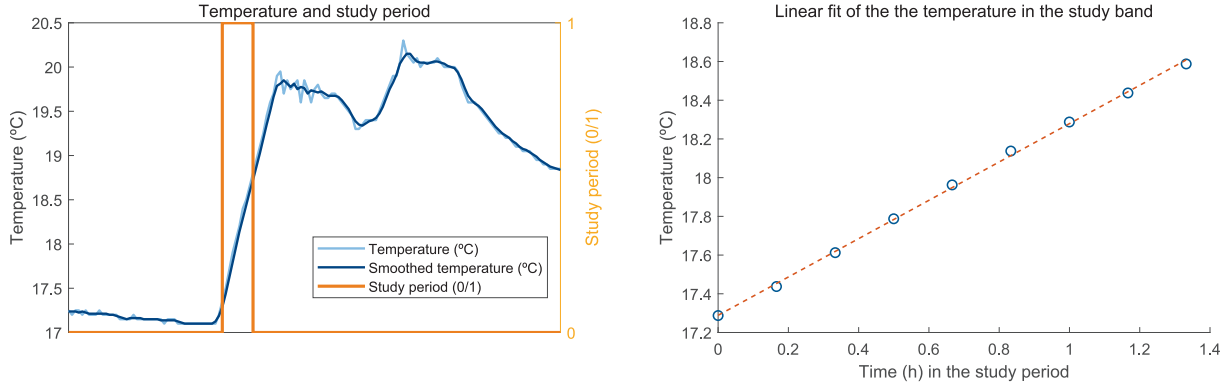

Fig. 3. A) temperature (°C) and study band for one day. B) linear fit of the temperature (°C) in the study band.

the detected "study band" and its corresponding linear fit. The search window for this start-up detection is defined from 4:00 a.m. to 9:00 a.m. This timeframe does not represent the duration of the event itself, but rather the designated period within which the program seeks to identify the actual, shorter study band (e.g., a specific ramp-up occurring between 5:30 a.m. and 9:00 a.m.). This early morning window is strategically selected to isolate the thermal contribution of the HVAC systems, thereby minimizing confounding internal gains from occupants, lighting, and other appliances. An example of this process applied over a two-week period is shown in Fig. 4, which plots the multiple study bands identified and their resulting slope and goodness-of-fit (R^2) values.

The program's methodology, shown schematically in Fig. 5, consists of a two-stage workflow: 1) start-up event detection and 2) slope calculation.

In the first stage, the raw measurements are loaded and pre-processed. First, timestamps are standardized to a common time zone to ensure temporal consistency across all sensors. To remove potentially spurious readings and guarantee physical plausibility, a domain-specific

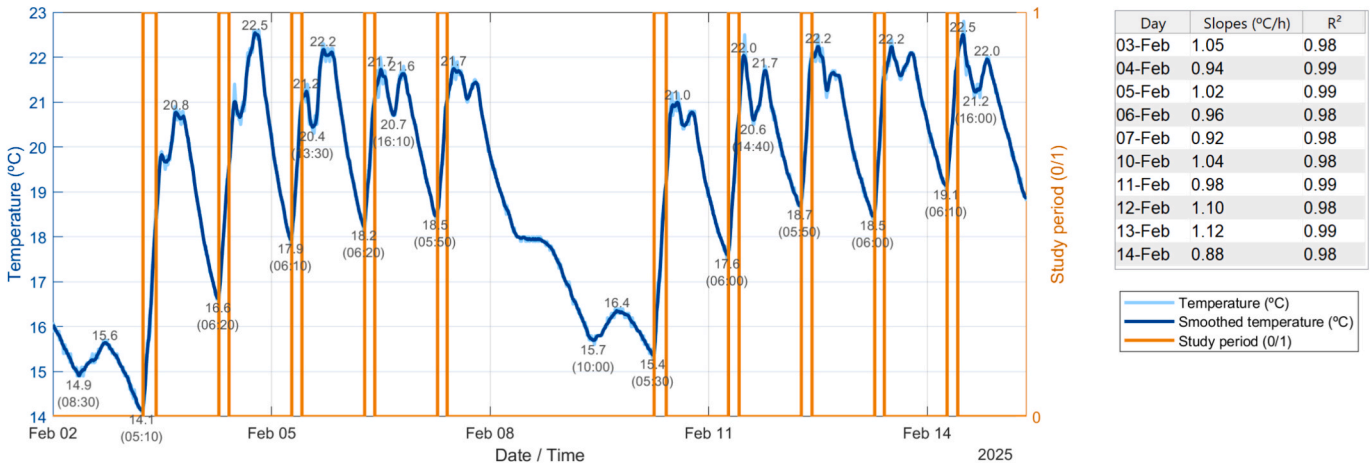

Day	Slopes (°C/h)	R^2
03-Feb	1.05	0.98
04-Feb	0.94	0.99
05-Feb	1.02	0.99
06-Feb	0.96	0.98
07-Feb	0.92	0.98
10-Feb	1.04	0.98
11-Feb	0.98	0.99
12-Feb	1.10	0.98
13-Feb	1.12	0.99
14-Feb	0.88	0.98

Fig. 4. A) example of temperature (°C) and study band for two weeks. B) linear fit of the temperature (°C) in the study band.

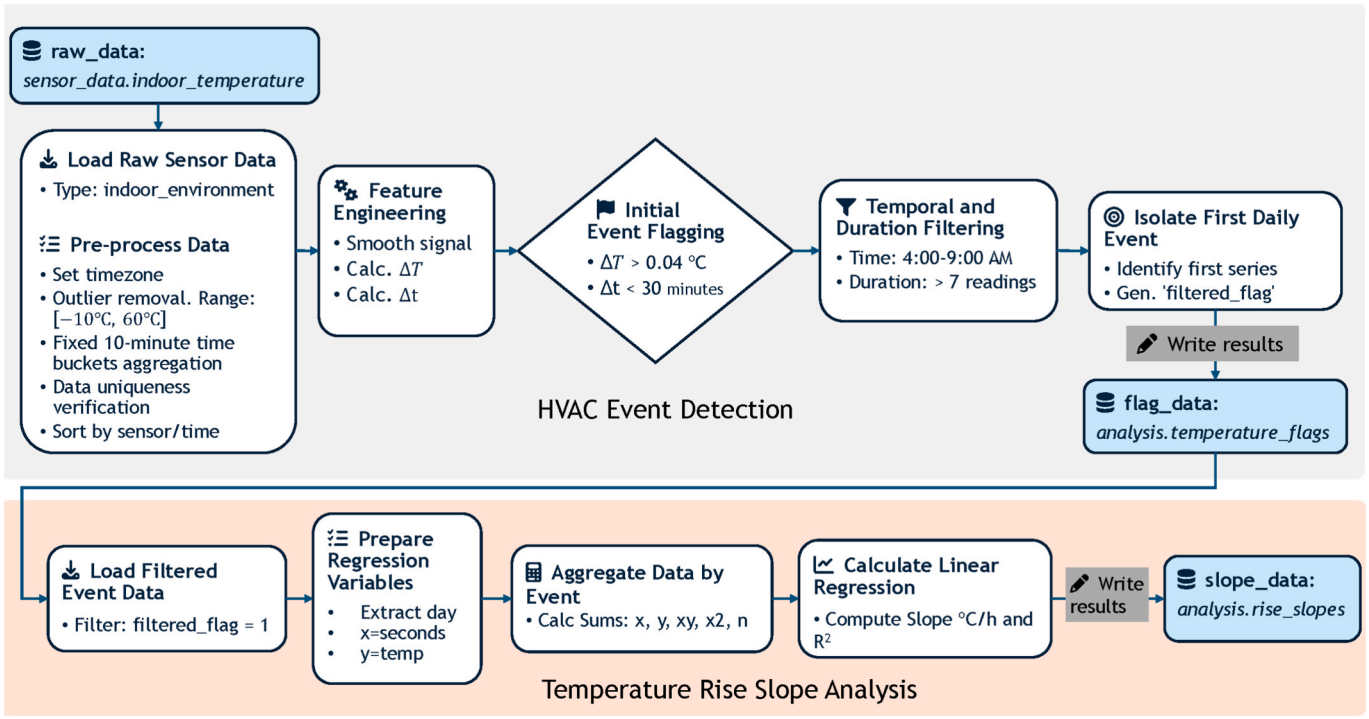

Fig. 5. Diagram of the calculation flow in Python.

filter restricts valid indoor air temperature values to the range $[-10^{\circ}C, 60^{\circ}C]$, discarding measurements outside this interval as outliers. Given the asynchronous nature of sensor transmissions, the filtered data are aggregated into fixed 10-minute time bins. To ensure a unique observation per sensor and time interval, any remaining duplicates are resolved by aggregation, yielding a single value per sensor and time bin. Finally, the resulting dataset is sorted by sensor and timestamp. It is worth noting that no correction for long-term sensor drift is performed; since the target metric is the differential heating slope ($\Delta T/\Delta t$), any constant calibration offset is effectively cancelled out, prioritizing short-term precision over absolute accuracy.

From this quality-controlled baseline, a secondary signal smoothing is applied via a 7-point rolling mean filter, to minimize numerical noise in the derivative calculation. Using this smoothed signal, the program performs an initial, sensitive detection: A preliminary flag is set if the temperature gradient (ΔT) exceeds 0.04 °C and the time difference (Δt) is less than 31 minutes. These thresholds for the detection algorithm were established based on the operational characteristics of the IoT monitoring infrastructure and the thermal dynamics of the buildings. Specifically:

Time gap ($\Delta t < 31$ min): To ensure robust event continuity despite the packet loss inherent to LoRaWAN networks. With a sampling interval (T_s) of 10 minutes, this window is specifically sized to tolerate the loss of two consecutive data packets ($3 \times T_s$) without artificially fragmenting a single heating event.
Gradient threshold ($\Delta T > 0.04^{\circ}C$): A value strictly calibrated to surpass the sensor quantization noise floor while maintaining high sensitivity. This threshold allows the algorithm to detect the earliest onset of the heating curve with minimal latency, distinguishing the active system response from random thermal fluctuations.
Consistency (≥ 7 consecutive readings): Given the 10-minute sampling rate, this constraint verifies a sustained temperature rise of 70 minutes. This duration effectively acts as a low-pass temporal filter,

rejecting short-term local disturbances to isolate the global thermal inertia driven by the HVAC system.

This preliminary flagging rule is intentionally sensitive. Therefore, a flag validation process is applied. This validation consists of two rules: 1) the event must occur within the 4:00 a.m. to 9:00 a.m. start-up window, and 2) a valid event must consist of at least 7 consecutive flagged readings. Critically, the program isolates only the first complete, validated heating event (*study band*) detected for that day.

This first stage runs once over the entire dataset (e.g., one year or more), identifying all valid daily study bands and saving them, marked with the *filtered_flag*, to an intermediate table (*analysis.temperature_flags*).

Following this, the second stage commences. It loads all the isolated study bands (i.e., where *filtered_flag* = 1) from the intermediate table. For each of these distinct events, the program fits the temperature data (y=temperature, x=seconds) to a line by calculating the necessary sums for a linear regression. This computation yields a definitive temperature rise slope (in °C/h) and its corresponding R^2 value. The final output is a comprehensive database table (*analysis.rise_slopes*) containing multiple calculated slopes for each sensor, one for each day a valid start-up event was detected, which is then used for further analysis.

This methodology employs a linear regression to model the zone temperature ramp-up during the pre-9 a.m. start-up period. Although the complete thermal response to a setpoint is physically a first-order exponential process, the analysis focuses on the initial pre-heating phase where the system operates far from the asymptotic steady state. As evidenced by representative temperature profiles (Fig. 6), this phase exhibits strong linearity, either due to the constant airflow in forced convection systems or the extended transient response of high-inertia emitters, which tend to rise monotonically throughout the occupancy period without reaching saturation. To guarantee the robustness of this approximation, a strict quality control filter has been implemented, retaining only those heating events with a coefficient of determination $R^2 \geq 0.9$, to ensure the calculated slope accurately reflects the system's active performance.

This methodological uncertainty (assessed by the R^2 goodness-of-fit) is acknowledged, alongside measurement uncertainty. However, it is important to note that the primary measurement concern is sensor precision (i.e., low noise) rather than absolute accuracy. Since the slope is derived from relative temperature changes, systematic sensor bias does not propagate into the rate calculation. This ensures the metric remains robust even if the sensor's absolute temperature reading is biased. While individual slopes are subject to noise and data integrity, the confidence in the average thermal response for a given zone is strengthened as the number of daily slopes captured over the analysis period increases.

Fig. 7 presents a diagram of the databases and their relationships, which are essential for conducting data analysis.

Using the calculation program developed in Python, the study focused on a 200-day interval covering the winter months of the 2024-2025 academic year. Throughout this period, new sensors were gradually installed, ultimately numbering 1500. Fig. 8 illustrates this timeframe and details the total number of data points processed.

3. Results and discussion

This section synthesizes the thermal analysis derived from the large-scale monitoring of 62 tertiary buildings. The discussion is structured to advance from qualitative causal characterization to quantitative validation and control application.

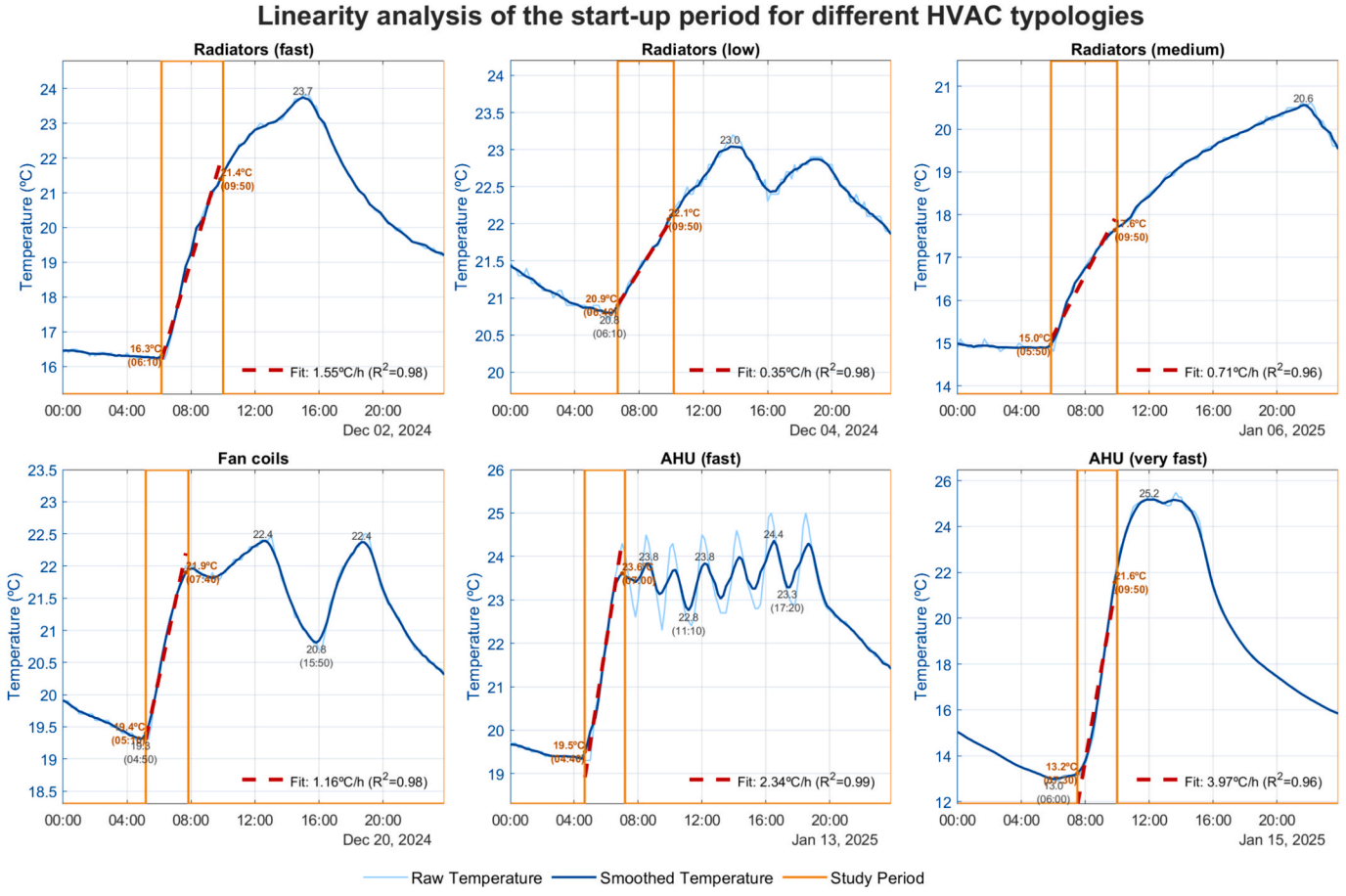

Fig. 6. Linearity analysis of the start-up period for different HVAC typologies.

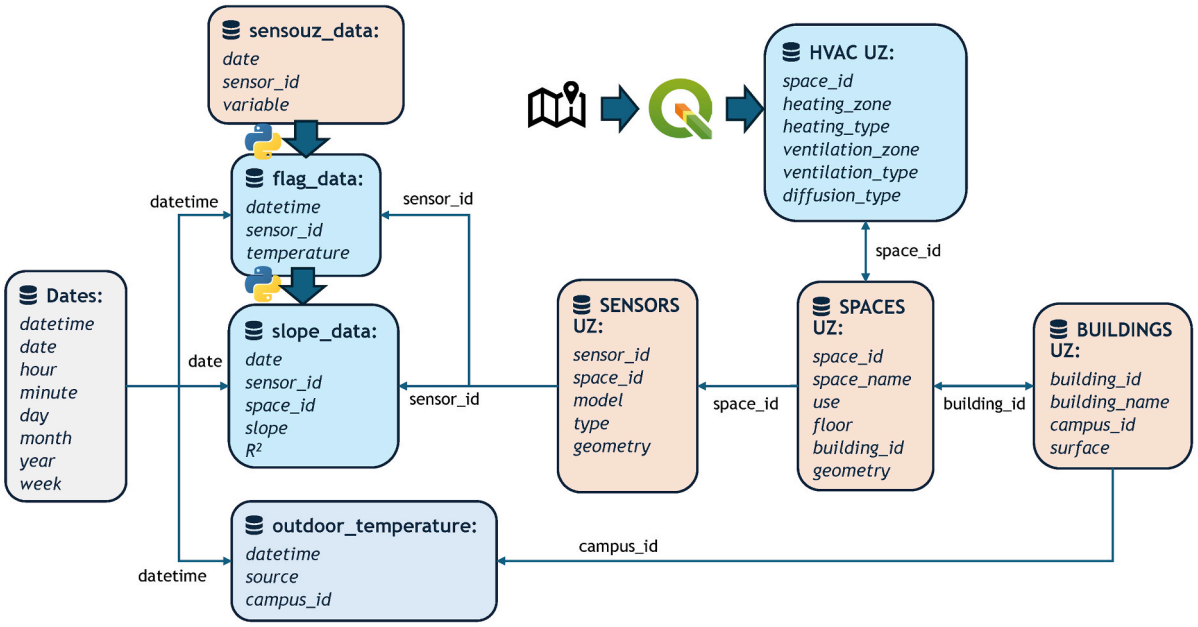

Fig. 7. Diagram showing databases and their joins.

Fig. 8. Key Study Metrics.

First, Section 3.1 (Statistical Characterization and Uncertainty Analysis) identifies the primary determinants of thermal response and applies this framework to the empirical dataset. This analysis adopts a hierarchical, multi-scalar approach, moving from a general building-level assessment down to specific zone (circuit) and space-level case studies. This progression demonstrates how spatial uncertainty can be mitigated to acceptable operational limits, provided the HVAC infrastructure offers sufficient zoning resolution.

Subsequently, Section 3.2 (Control Strategy and Field Validation) formulates the specific control methodology and details a real application case. This pilot study evaluates the system's performance in terms of thermal comfort compliance and energy efficiency improvements relative to the pre-implementation situation.

Finally, Section 3.3 (Methodological Boundaries and Limitations) outlines the operational scope, addressing constraints related to linearity, seasonal sensitivity, and zoning level to distinguish between algorithmic trade-offs and physical retrofitting requirements.

3.1. Statistical Characterization and Uncertainty Analysis

As a preliminary analysis, the average thermal response rate was calculated at the building level for the 2024-2025 winter heating season. The dataset comprises a total of nearly 62,000 valid study bands (heating intervals), with the sample size for each building determined by the extent of sensor deployment and the frequency of HVAC activations. These values represent the aggregate behaviour derived from all sensors and detected curves. To ensure a robust characterization that accounts for the dispersion observed in such a large dataset, the analysis relies on the following statistical definitions:

Let $m_{i,t}$ be the heating slope (in °C/h) calculated for:

- Sensor i (where $i = 1, \cdots, N_s$, with N_s being the number of sensors in the building).
- Day t (where $t = 1, \cdots, N_d$, with N_d being the number of valid days analysed).

Average slopes per building: Represents the nominal thermal behaviour of the building ($\mu_{building}$), defined as the overall average of all valid observations:

$$\mu_{building} = \frac{1}{N_s}\sum_{i=1}^{N_s}\left(\frac{1}{N_d}\sum_{t=1}^{N_d} m_{i,t}\right)$$

Temporal Uncertainty ($\sigma_{temporal}$): This component captures the temporal variability associated with transient boundary conditions and the progressive evolution of the system. On the demand side, it accounts for meteorological variability such as outdoor temperature and wind intensity, as well as the initial indoor temperature linked to thermal inertia and recurring patterns related to the day of the week. On the supply side, uncertainty arises from variations in supply temperatures, changes in control and regulation strategies, and system ageing, which accounts for both long-term component degradation and sudden performance changes due to equipment replacement.

When considering sensors in a zone, it is calculated by first obtaining the temporal variance of each sensor $\left(\sigma_i^2\right)$ and then averaging it for the building.

Average slopes for each sensor:$\overline{m}_i = \frac{1}{N_d}\sum_{t=1}^{N_d} m_{i,t}$

Variance of each sensor:$\sigma_i^2 = \frac{1}{N_d-1}\sum_{t=1}^{N_d}\left(m_{i,t} - \overline{m}_i\right)^2$

$$\sigma_{temporal} = \sqrt{\frac{1}{N_s}\sum_{i=1}^{N_s}\sigma_i^2}$$

Spatial Uncertainty ($\sigma_{spatial}$): It represents the dispersion between the different zones of the building, driven by multiple factors, including spatial location relative to solar irradiation and wind incidence, building envelope characteristics, and stochastic events. However, the heterogeneity of the HVAC system itself acts as a primary determinant of this variability. Significant discrepancies arise from the specific technology employed (e.g., air-based vs. water-based systems) and the hydraulic circuit architecture. The thermal response can differ substantially depending on the specific loop assignment, the circuit length, and the position of the space within the hydraulic branch (beginning vs. end). At the room level, the configuration of terminal units, including their dimensions and real-time regulation strategies, such as the degree of valve opening or fan power settings, further determine the thermal behaviour.

$$\sigma_{spatial} = \sqrt{\frac{1}{N_s-1}\sum_{i=1}^{N_s}\left(\overline{m}_i - \mu_{building}\right)^2}$$

Table 3 summarises the factors influencing variations in slopes between buildings, between spaces within a building, and over time.

Building-Level Analysis

Table 4 presents the average heating slopes derived from all sensors and valid events within each building. This analysis highlights significant inter-building variability, with rates ranging from 0.3 to 3.0 °C/h on average per month. Based on this average slope, buildings were classified into performance categories, ranging from "A" (very fast, >2.0°C/h) to "F" (very slow, <0.6°C/h). Such heterogeneity, driven by the HVAC power-to-demand ratio, system typology, and operational settings, demonstrates that a uniform campus-wide schedule is ill-suited to the unique dynamics of each facility. As outlined in Table 4, the level of uncertainty varies significantly across the portfolio. Certain facilities, such as the Faculty of Veterinary Medicine (Zootechnics), demonstrate thermal homogeneity. Conversely, the Faculty of Education exhibits high uncertainty, driven largely by significant spatial heterogeneity. This variation stems from the presence of distinct thermal zones controlled by separate HVAC systems, underscoring the limitations of a global building-level metric and justifying a more detailed, zone-based analysis.

Zone-Level Analysis

In view of these findings, further analysis at the zone level was conducted, with zones defined according to their associated HVAC control circuits and terminal units (e.g., radiators, fan coils, Air Handling Units (AHUs), and radiant flooring).

This zonal characterization is a detailed process: First, an analysis of the building's hydraulic circuits is performed to identify if zoning by floor or system type (e.g., radiators, fan coils) exists. Second, as-built installation plans or subsequent reform project documents are verified to identify the zones affected by each circuit. Third, this information is used to update the University's central space database, tagging each room with new attributes such as its specific circuit and terminal unit type. Because all sensors are already linked to these spaces, this database enrichment automatically enables the aggregation and analysis of thermal slopes by these new, physically defined zones, as illustrated in Fig. 7.

A case study of this zonal approach for the Faculty of Education is presented in Fig. 9. After identifying these distinct HVAC zones, the monthly average slope for the sensors within each zone was calculated, as shown in Table 5. AHUs provide the fastest thermal response, followed by fan coils and radiators. This zone-level characterization provides a better level of detail for the proposed dynamic control model. Although, if the building allows it, zoning at the space level reduces uncertainty and improves control.

This zonal analysis methodology has been extended to a larger number of buildings, enabling the quantification and classification of systems based on their thermal response. The following ranking, from fastest to slowest measured response, is as follows: Air Handling Units (AHUs) (~1-3 °C/h), floor fan coils (~1-2.5 °C/h), ceiling fan coils (~0.8-1.4 °C/h), conventional radiators (~0.6-1.4 °C/h), underfloor heating (~0.5-0.6 °C/h), and radiant ceilings (~0.5 °C/h).

These results empirically corroborate that forced convection systems (AHUs and fan coils) are the most rapid, driven by the mechanically induced airflow that maximizes the convective heat transfer coefficient (h_c) and ensures immediate air mixing. In contrast, conventional radiators rely on natural convection, requiring a larger temperature differential to establish effective air circulation. The significant variation observed within the radiator category reflects the combined influence of two structural factors: the emitter's thermal mass and the installed power-to-demand ratio. Undersized zones naturally exhibit a more sluggish rise, regardless of the material. Finally, high-inertia radiant systems are the slowest. Underfloor heating must first absorb energy to heat the structural mass, creating an inherent lag. Radiant ceilings, while faster to heat up the surface, suffer from stratification: since heat is introduced from the top, warm air remains trapped at ceiling level. This results in a delayed detection by wall-mounted sensors compared to convective systems, where air mixing is more efficient.

Room-Level Analysis

To characterize the thermal response at the finest spatial scale (room level), the Faculty of Philosophy and Humanities was selected as a specific case study. This complex consists of two connected structures: the Central Building (recently rehabilitated) and the Departmental Building (newly constructed). Following recent retrofitting, the facility is equipped with temperature sensors installed in each individual space, and the BMS could support the implementation of a customised start-up sequence governed by a critical-zone logic, whereby the areas exhibiting the most unfavourable thermal condition determine the master start command. This command would initiate the operation of the central generation unit and the associated primary and secondary hydraulic pumps, while activating only the terminal units serving the identified critical zones.

Figs. 10 and 11 detail the thermal response for the Central and Departmental buildings respectively. The analysis reveals distinct

Table 3
Main factors influencing the value of the slopes.

Variations in slopes over time	**Indoor temperature** (day of the week)
	Outdoor temperatures
	Change in installations: Ageing or new equipment.
	Varying HVAC control settings
Variations between spaces on the same day and building	Multiple HVAC system in the building: Air handling unit, fan coils, radiators, etc.
	Nature of enclosures
	Orientation and floor level with respect to solar irradiation and wind incidence
Differing behaviours of buildings	**Ratio of HVAC installed capacity to thermal demand**
	HVAC system: Primary and secondary
	Building use (teaching, research, study rooms, halls of residence, etc.)

Table 4
Categories for the classification of buildings, according to the average heating rate in °C/h in the winter months of 2024–25.

Group	Campus	Building name	$\mu_{building}$	$\bar{\sigma}_{\text{temporal}}$	σ_{spatial}	N^{o} sensors	N^{o} slopes
A >2 °C/h	CSF	Central Services	2.17	0.72	0.48	7	690
A >2 °C/h	CSF	Faculty of Philosophy and Humanities - Geography Pavilion	2.03	0.68	0.51	32	516
B (1.5-2] °C/h	CHU	Faculty of Veterinary Medicine - Pilot Plant - Food Science and Technology	1.85	0.47	0.26	2	127
B (1.5-2] °C/h	CMS	Interfaculties III. Doctoral School and Study Hall	1.77	0.62	0.00	1	34
B (1.5-2] °C/h	CRE	CIUR - Information, OUAD - Diversity Support, Travel	1.70	0.54	0.53	4	163
B (1.5-2] °C/h	CSF	Faculty of Law - Law Building II	1.61	0.18	0.22	5	339
B (1.5-2] °C/h	CSF	EINA - Torres Quevedo	1.57	0.39	0.63	57	1332
B (1.5-2] °C/h	CSF	Faculty of Business and Public Management - Former children's home	1.48	0.62	0.38	11	748
C (1-1.5] °C/h	CHU	Vice-Rectorate of Huesca	1.41	0.50	0.17	6	226
C (1-1.5] °C/h	CHU	Construction and Maintenance Building - UTCM	1.41	0.47	0.52	13	505
C (1-1.5] °C/h	CHU	SAI - Warehouse N 5 - SAEA Offices	1.36	0.38	0.16	6	864
C (1-1.5] °C/h	CHU	Faculty of Social and Labour Sciences	1.34	0.51	0.76	15	1084
C (1-1.5] °C/h	CHU	Vice-Rectorate of Teruel	1.30	0.34	0.68	8	627
C (1-1.5] °C/h	CHU	Faculty of Economics and Business - Lorenzo Normante	1.27	0.39	0.33	20	1389
C (1-1.5] °C/h	CMS	Faculty of Education	1.24	0.46	0.64	23	1161
C (1-1.5] °C/h	CMS	Faculty of Law - Law Building III	1.23	0.42	0.52	19	1402
C (1-1.5] °C/h	CPE	Faculty of Philosophy and Humanities - Central Pavilion	1.23	0.36	0.56	119	1705
C (1-1.5] °C/h	CPE	Faculty of Economics and Business - Library	1.21	0.39	0.48	10	711
C (1-1.5] °C/h	CRE	Faculty of Humanities and Education - Main Building	1.21	0.58	0.59	21	1141
C (1-1.5] °C/h	CRE	Faculty of Economics and Business - Great Hall	1.19	0.47	0.19	6	422
C (1-1.5] °C/h	CRE	Faculty of Medicine - Building A	1.18	0.40	0.43	20	979
C (1-1.5] °C/h	CSF	E.P.S. - Laboratories - Loreto Building	1.17	0.54	0.49	3	325
C (1-1.5] °C/h	CSF	Universa	1.12	0.43	0.36	6	100
C (1-1.5] °C/h	CSF	Jaca Residence Building	1.09	0.18	0.24	13	125
C (1-1.5] °C/h	CSF	SAI Building - Research Support Service	1.09	0.48	0.45	6	393
C (1-1.5] °C/h	CSF	Faculty of Veterinary Medicine - Lecture Hall Building	1.04	0.35	0.53	12	835
C (1-1.5] °C/h	CSF	R&D - Research Institutes	1.02	0.68	0.45	11	313
C (1-1.5] °C/h	CSF	Faculty of Law - Law Building I	1.00	0.35	0.76	12	888
C (1-1.5] °C/h	CSF	E.P.S. - Polytechnic - Tozal de Guara Building	1.00	0.34	0.50	12	690
C (1-1.5] °C/h	CSF	Faculty of Health Sciences	0.94	0.41	0.36	16	1220
C (1-1.5] °C/h	CTE	Faculty of Humanities and Education - Annex	0.91	0.28	0.00	2	65
D (0.8-1] °C/h	CHU	Faculty of Health and Sport Sciences - Dentistry Building	0.89	0.21	0.14	4	386
D (0.8-1] °C/h	CHU	Faculty of Health and Sport Sciences - Rio Isuela Sports Complex	0.88	0.37	0.46	17	911
D (0.8-1] °C/h	CHU	E.P.S. - Classrooms - Gratal Building	0.88	0.24	0.16	2	154
D (0.8-1] °C/h	CMS	EINA - Ada Byron	0.88	0.30	0.33	76	4338
D (0.8-1] °C/h	CRE	Center for Innovation, Training, and Research in Educational Sciences	0.88	0.24	0.23	6	510
D (0.8-1] °C/h	CSF	University Sports Pavilion - SAD	0.87	0.30	0.24	19	906
D (0.8-1] °C/h	CSF	EINA - Betancourt	0.87	0.29	0.27	51	2428
D (0.8-1] °C/h	CSF	Interfaculties I	0.85	0.23	0.26	24	2193
D (0.8-1] °C/h	CSF	Faculty of Sciences - Building D - Chemistry	0.84	0.26	0.30	24	576
D (0.8-1] °C/h	CSF	Faculty of Veterinary Medicine - Veterinary Hospital Building	0.82	0.26	0.29	28	608
D (0.8-1] °C/h	CSF	Faculty of Medicine - Building B	0.81	0.28	0.22	13	1029
E (0.6-0.8] °C/h	CHU	Pablo Serrano Residence Hall	0.78	0.25	0.40	180	7084
E (0.6-0.8] °C/h	CHU	Cervantes Building - Faculty of Philosophy and Humanities	0.76	0.17	0.14	7	556
E (0.6-0.8] °C/h	CMS	Faculty of Philosophy and Humanities - Pavilion B	0.75	0.18	0.33	188	2236
E (0.6-0.8] °C/h	CPE	Faculty of Veterinary Medicine - Central Building	0.75	0.20	0.19	16	992
E (0.6-0.8] °C/h	CSF	Faculty of Social Sciences and Humanities	0.75	0.20	0.16	15	1511
E (0.6-0.8] °C/h	CSF	Faculty of Sciences - Building B - Mathematics	0.72	0.22	0.17	22	1703
E (0.6-0.8] °C/h	CSF	E.P.S. - Chalets - Salto del Roldán Building	0.71	0.17	0.14	5	296
E (0.6-0.8] °C/h	CSF	Faculty of Economics and Business	0.70	0.20	0.19	35	2331
E (0.6-0.8] °C/h	CTE	Faculty of Health and Sport Sciences and Ramon Acín Residence Hall	0.65	0.26	0.19	16	848
E (0.6-0.8] °C/h	CTE	Faculty of Sciences - Building A - Physics	0.62	0.15	0.07	15	1289
E (0.6-0.8] °C/h	CTE	Fine Arts	0.61	0.15	0.16	16	1204
F <0.6 °C/h	CMS	Cerbuna Residence Hall	0.59	0.14	0.13	27	722
F <0.6 °C/h	CPE	Faculty of Sciences - Building C - Geology	0.57	0.17	0.11	16	1024
F <0.6 °C/h	CSF	Faculty of Philosophy and Humanities - Humanities Library	0.56	0.14	0.11	8	476
F <0.6 °C/h	CSF	Polytechnic University School of Teruel	0.55	0.11	0.07	21	1923
F <0.6 °C/h	CSF	Faculty of Veterinary Medicine - Zootechnics Building	0.52	0.12	0.09	29	1360
F <0.6 °C/h	CSF	Professors' Residence (or Faculty Residence)	0.49	0.12	0.07	6	530

thermal performance, both between the two main buildings and within them.

The offices of the Central Building, for example, exhibit a much higher heating rate than those of the Departmental Building. Furthermore, significant variations exist within each structure. The Central Building displays a clear performance hierarchy: its two office wings are the fastest to heat, followed by the classroom zones, with the central hallway being the slowest. Similarly, the Departmental Building consists of three distinct office zones and a classroom area, each exhibiting different thermal responses. The left-side offices heat up slightly faster than those on the right, while the classroom area shows a significantly higher response rate compared to all office zones.

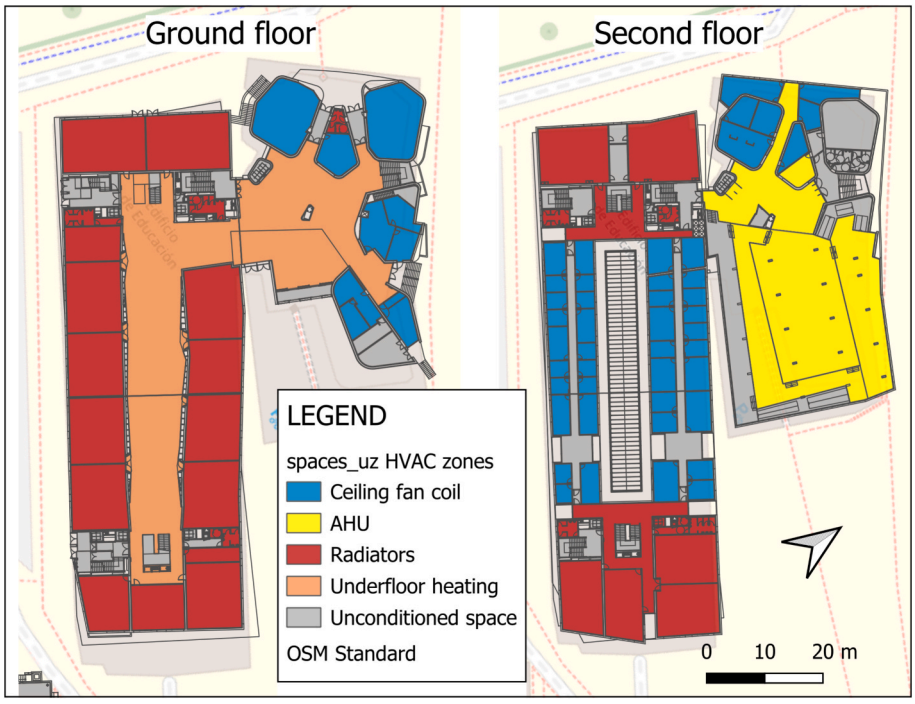

Fig. 9. HVAC terminal units by zone (ground floor and second floor). Faculty of Education.

Table 5
Average heating rate in °C/h by month and zone and $\sigma_{spatial}$. Faculty of Education.

HVAC system	11/2024	12/2024	1/2025	2/2025	3/2025	Average slopes [°C/h]
Fancoils	0.77 ±0.18	1.16 ±0.34	1.12 ±0.55	1.02 ±0.42	0.97 ±0.37	1.04
Radiators (Circuit 2)	1.08 ±0.31	1.03 ±0.58	0.93 ±0.15	0.97 ±0.13	1.11 ±0.27	1.01
Radiators (Circuit 3)	0.88 ±0.12	0.8 ±0.13	0.85 ±0.22	0.88 ±0.12	0.86 ±0.10	0.85
Air Handling Unit (1)	3.2 ±0.07	2.5 ±0.42	3.05 ±0.60	3.02 ±0.62	2.59 ±0.03	2.87

By isolating the analysis to individual spaces, spatial heterogeneity in the output variable (slope) is effectively removed, leaving temporal variability as the dominant source of uncertainty. This downscaling from the building level to the zone or space level, when supported by a physically zoned HVAC infrastructure, substantially reduces uncertainty and enables more precise control strategies.

Impact of Boundary Conditions

Temporal variability was subsequently analysed using several approaches, including average slope values over the study period, slope values corresponding to the same weekday of the previous week, and an empirical multivariable correlation model based on indoor temperature, outdoor temperature, and day of the week.

To quantify the influence of environmental and operational boundary conditions on the system's performance, a multivariable linear regression was conducted in which the heating ramp-up slope (m) was expressed as a function of the initial indoor temperature ($T_{i,start}$), the outdoor temperature ($T_{out,start}$), and a binary temporal variable representing the start of the week (D_{mon}), according to:

$$m = \beta_0 + \beta_{in} \cdot T_{i,start} + \beta_{out} \cdot T_{out,start} + \beta_{mon} \cdot D_{mon}$$

The coefficients of determination (R^2) averaged 0.3 across the analysed buildings, with values ranging from 0.05 to 0.6. This relatively low explanatory power indicates that instantaneous temperature variables ($T_{i,start}$, $T_{out,start}$) account for only approximately 30% of the variance in heating speeds. The remaining unexplained variance suggests that unmodeled stochastic factors, such as wind speed, infiltration rates, and variable hydraulic balancing, play a dominant role in the transient heating process.

The standardized regression coefficients revealed that the initial indoor temperature (β_{in}) is consistently a stronger predictor of the heating slope than the outdoor temperature (β_{out}). From a physical perspective, $T_{i,start}$ effectively acts as a proxy for the zone's recent thermal history, integrating the cumulative effect of external conditions over time. This implies that the start-up dynamics are governed primarily by the internal thermal potential rather than by instantaneous envelope heat losses, as illustrated in Fig. 12.

Although β_{out} is theoretically expected to be positive, as higher outdoor temperatures reduce envelope heat losses and facilitate faster heating, an opposite trend is observed in some cases. This counterintuitive behaviour, where colder outdoor conditions correlate with steeper heating slopes, can be attributed to two concurrent mechanisms. First, these situations often coincide with particularly low initial indoor temperatures, resulting in a dominant internal thermal gradient ($\Delta T_i = T_{emitter} - T_{i,start}$). According to the law of convection, this increased temperature difference maximizes convective heat transfer from the

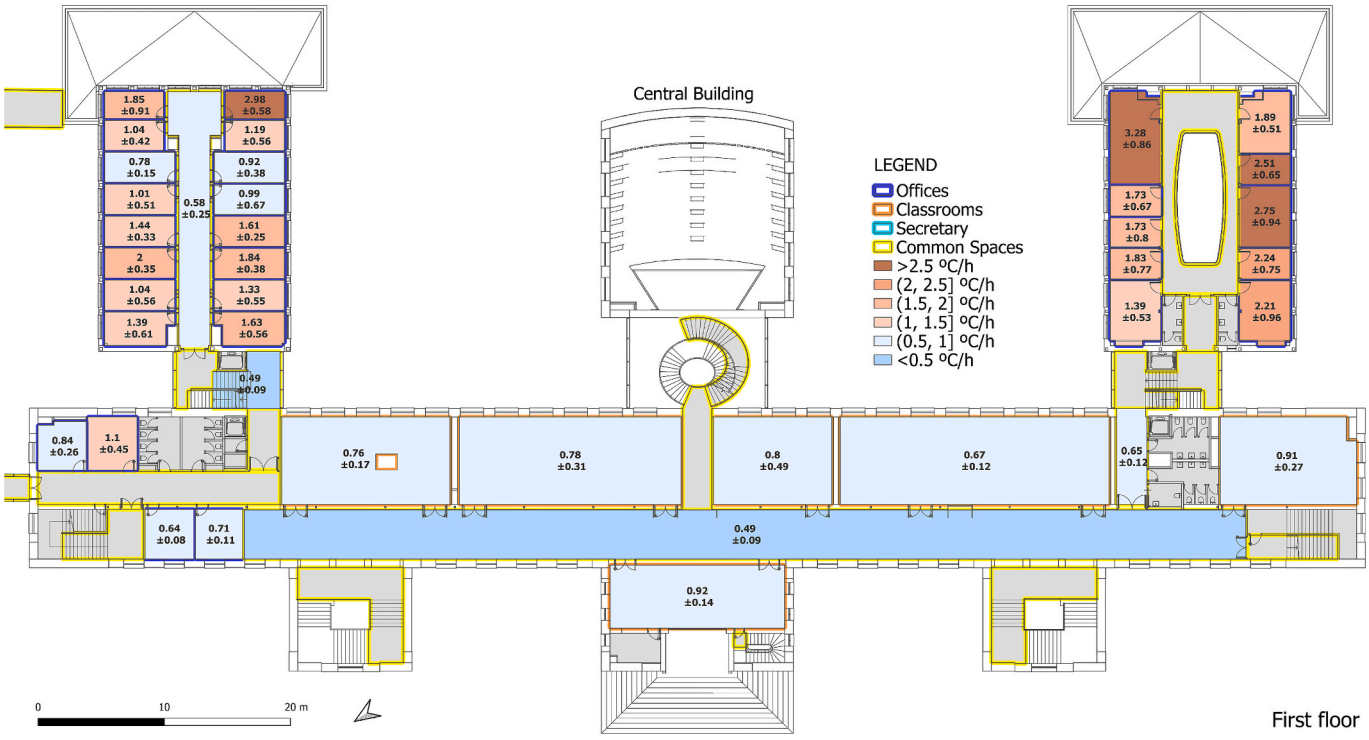

Fig. 10. Average heating rate in °C/h per space in the Faculty of Philosophy and Humanities. Central Building.

emitters, outweighing the effect of increased envelope losses. Second, the negative correlation suggests a response of the BMS in certain installations, where low outdoor or return water temperatures activate hydraulic compensation strategies that significantly increase supply water temperatures and injected thermal power compared to mild weather operation.

Finally, the coefficient for Mondays (β_{mon}) quantifies the impact of intermittency. It is predominantly negative, reflecting structural thermal hysteresis. After the weekend shutdown, the building's deep thermal mass acts as a significant heat sink, absorbing a portion of the thermal load via radiation and slowing the rise of the air temperature compared to continuous operation days.

Based on the results of this analysis and considering the influencing factors identified in Table 3, the difference between the average based approach and the empirical regression model is marginal and does not currently justify the additional complexity of the latter. The weekday-based approach performs worse, likely due to its reliance on single reference values.

3.2. Control Strategy and Field Validation

Based on this study of thermal response, a new methodology is proposed to dynamically determine the real-time operation of HVAC systems. This methodology is currently being implemented in the SCADA system and tested in several buildings at the University of Zaragoza.

The data-driven model developed in this study is integrated into a new management framework based on three distinct time schedules. The first is the Occupancy Schedule, which corresponds to the building's official opening hours. During this period, thermal comfort conditions must be guaranteed, with the indoor temperature required to be at least 19°C at both the beginning and end of the schedule. The most representative sensors from the "campusFiDigital" infrastructure are used as the reference for temperature control, as illustrated in Fig. 14. The second schedule is the HVAC Schedule, a variable and dynamic window determining when heating production is active, adjusted based on current indoor temperature and the thermal response of the zone. The third is the Security Schedule, a fixed "safe" period (e.g., 4:00 a.m. to 9:00 p.m.) within which the dynamic "HVAC Schedule" must always be contained.

Based on this framework, the operational logic begins before the Occupancy Schedule, when heating production and distribution are activated (preheating) with sufficient anticipation to reach the 19°C target precisely at the start of occupancy. During the Occupancy Schedule, the system modulates to maintain the indoor temperature around the primary comfort setpoint (e.g., 21°C). At the end of the Occupancy Schedule, the production (boilers/heat pumps) is shut down, but circulation pumps remain active to leverage residual heat in the circuit. The pumps are only deactivated once the water cools, ensuring the indoor temperature remains above the 19°C minimum at the designated end time.

This management framework is automated by the data-driven model, which is integrated directly into each building's PLC (Programmable Logic Controller). The model dynamically calculates the optimal pre-conditioning time ($\Delta t_{preheat}$) required for each zone, and the resulting schedules are graphically represented on the central SCADA interface. The model's objective is to ensure the 19°C target is met precisely at the start of the Occupancy Schedule, minimizing energy waste from premature start-ups.

The model utilizes the zone-specific thermal response rate ($Slope_{zone}$, in °C/h) calculated as the aggregate average of all valid heating slopes derived from the historical "study bands" across all sensors within that zone. When the system evaluates a potential start-up (within the "Security Schedule"), it queries the current indoor temperature ($T_{current}$). The required temperature lift (ΔT_{lift}) is then calculated as the difference between the occupancy-start target ($T_{target} = 19^{\circ}C$) and the current temperature. The necessary preheat time is determined using the core equation of the model:

$$\Delta t_{preheat} = \frac{\Delta T_{lift}}{Slope_{zone}} = \frac{T_{target} - T_{current}}{Slope_{zone}}$$

The dynamic "HVAC Schedule" is then initiated by activating the system at the optimal start time (T_{start}), calculated by subtracting this required preheat time from the Occupancy Schedule start time

Fig. 11. Average heating rate in °C/h per space in the Faculty of Philosophy and Humanities. Departmental Building.

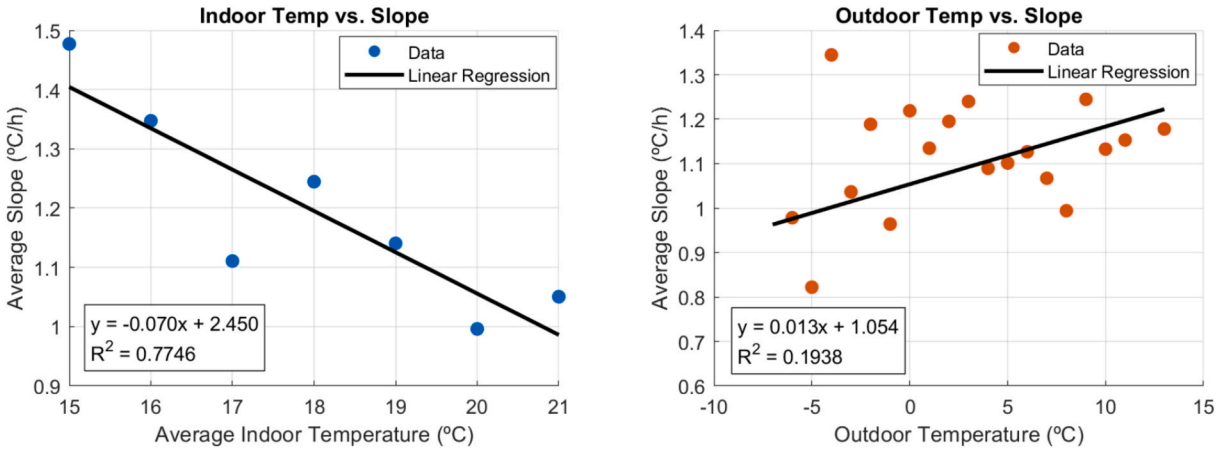

Fig. 12. Example of regression analysis between slope values and indoor or outdoor temperature at the time of HVAC start-up.

($T_{occupancy}$):$T_{start} = T_{occupancy} - \Delta t_{preheat}$

This approach entails a transition from a uniform, forecast-based schedule of HVAC control to one that is instead adaptive and measurement-driven. The latter is a strategy that is tailored to the unique thermal response of each individual zone.

The functionality of the system is illustrated in Fig. 13, which depicts an example scenario with an Occupancy Schedule of 8:00–21:00 and a Security Schedule of 4:00–21:00. The figure highlights the dynamic preheating phase, calculated to precisely meet the 19°C minimum comfort temperature at the 8:00 start time. During occupancy, the system would then modulate around a primary comfort setpoint (e.g., 21°C).

Furthermore, the framework is designed to incorporate cooling decay calculations. Although not the object of this paper, this development would allow the system to anticipate the production shutdown, coasting to the 19°C minimum target precisely at the end of the Occupancy Schedule, thus optimizing energy savings.

In older buildings where thermal segmentation is not feasible, selecting representative sensors is critical for optimal HVAC system performance and preventing localized overheating or cold zones. To address this, a Python script was developed to quantify sensor deviation.

The script operates by first identifying days with detected HVAC activation within each building. For these active periods, it calculates the building's mean temperature at each timestamp using a window function. The deviation of each individual sensor is then determined by subtracting this building-wide average from the sensor's specific reading.

This data is aggregated by *building_id*, date, and *sensor_id* to compute the *avg_daily_deviation*. This metric quantifies the sensor's average daily bias (i.e., its tendency to read warmer or cooler than the mean). As an example, Fig. 14 shows these daily bias values grouped by month for a specific building.

The evaluation of the proposed methodology is illustrated by the thermal behaviour of one of the analysed buildings. Fig. 15 displays the temperature evolution and demand state during a week before the implementation of the proposed control system, while Fig. 16 shows the results after implementation, under similar environmental conditions. The operational data reveals a transition from a rigid to a dynamic regime: whereas Table 6 (left) shows a fixed start-up time under conventional control, Table 8 (left) demonstrates the adaptive nature of the methodology, showing how the optimal HVAC start-up time is dynamically adjusted daily. This is reflected in the variation of the start time throughout the week, which ranged from 4:00 a.m. on Monday to 7:50 a.m. on Friday.

As shown in Table 8 (right), the primary control objective, reaching the desired indoor temperature setpoint of 19°C by the 8:00 a.m. occupancy time, was successfully achieved on most days. A notable exception occurred on Monday, when the target temperature was not met. This was due to a pre-set safety constraint within the BAC system, which limits the earliest possible startup to 4:00 a.m. On this particular day, the combination of low outdoor temperatures and the building's thermal inertia from the weekend shutdown required a preheat time longer than this safety limit allowed.

Furthermore, Fig. 16 shows how the implemented methodology modulates the secondary circuit pumps during occupation. The control strategy deactivates the pumps when the temperature exceeds the upper setpoint of 22°C, operating with a hysteresis of ±0.5°C. On Monday, specifically, the pumps did not disconnect during the entire HVAC schedule. This is consistent with the insufficient preheating time resulting from the 4 a.m. safety constraint, as the system was continuously working to reach the comfort range.

This approach significantly differs from the behaviour observed in Fig. 15, where the pumps run continuously without modulation, causing the building to overheat. To quantify this improvement, Table 7 and Table 9 present the percentage distribution of indoor air temperature ranges during occupancy hours before and after the implementation of the proposed control system, respectively. Table 9 indicates a significant decrease in overheating occurrences, ensuring comfort and energy efficiency. Furthermore, the implementation of the methodology successfully reduced the total activation time from 46.00 hours to 38.21 hours, resulting in a 16.93% reduction in system runtime.

Based on this preliminary validation, ongoing research, the detailed results of which will be presented in a forthcoming publication, focuses on the large-scale implementation of the integrated HVAC management system, supported by IoT and Spatial Data Infrastructure (SDI) technologies, across the university campus. This comprehensive case study aims to rigorously assess the system's performance under real operating conditions, with particular emphasis on quantifying variations in energy consumption and evaluating improvements in thermal comfort. Furthermore, the system's diagnostic potential is being investigated to proactively identify building zones requiring maintenance or improved thermal zoning, thereby contributing to the refinement of the

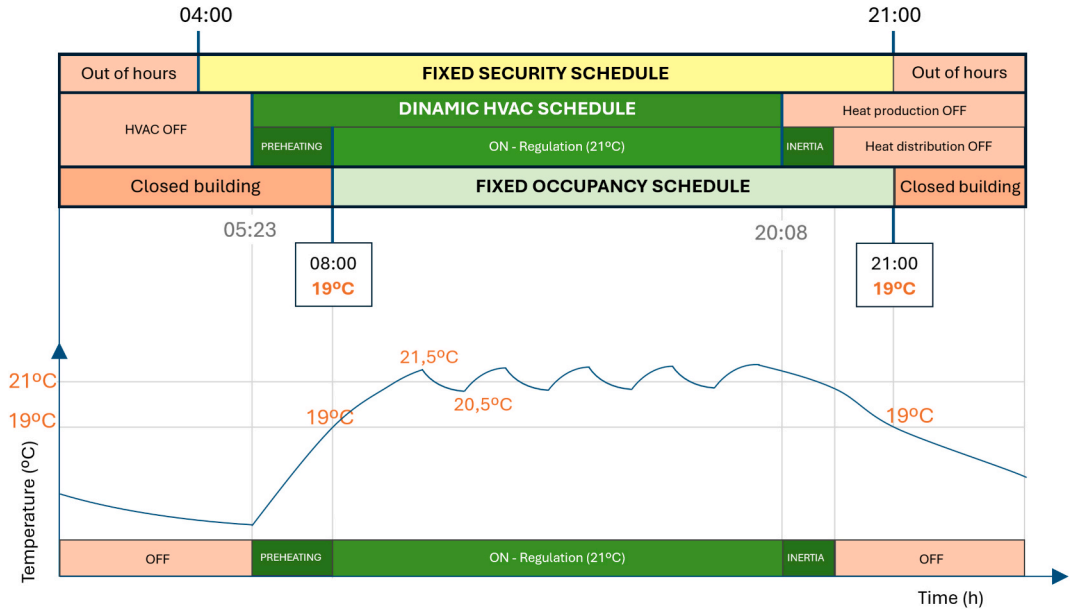

Fig. 13. Heating mode HVAC system management diagram. Temperature evolution is shown as an example.

sensor_id	10/2024	11/2024	12/2024	01/2025	02/2025	03/2025	Average
CTE.1150.03.290.SAR.BUA001	1.21	1.04	1.99	1.87	2.33	1.84	**1.74**
CTE.1150.00.210.SAR.BUA001	1.43	1.97	1.95	1.62	1.16	1.64	**1.61**
CTE.1150.03.360.SAR.BUA001	0.86	0.95	1.56	1.89	2.46	1.45	**1.60**
CTE.1150.02.060.SAR.BUA001	0.86	1.17	1.61	1.71	2.15	1.29	**1.52**
CTE.1150.02.260.SAR.BUA001	1.12	1.34	1.24	1.52	2.13	0.62	**1.37**
CTE.1150.00.230.SAR.BUA001	0.84	1.31	1.21	1.09	0.89	1.15	**1.08**
CTE.1150.02.220.SAR.BUA001	-0.29	0.35	0.78	0.86	0.92	0.77	**0.62**
CTE.1150.03.090.SAR.BUA001	0.37	-0.07	1.18	0.99	0.48	-0.20	**0.41**
CTE.1150.02.110.SAR.BUA001	-0.38	0.10	-0.05	0.54	0.21	1.20	**0.34**
CTE.1150.01.160.SAR.BUA001	0.04		0.04	0.59	-0.06	0.79	**0.31**
CTE.1150.00.140.SAR.BUA001	0.76	0.68	0.14	-0.07	-0.12	-0.03	**0.19**
CTE.1150.01.200.SAR.BUA001	-0.41	0.40	0.54	0.18	-0.30	-0.20	**0.02**
CTE.1150.01.090.SAR.BUA001	-0.49	-0.25	-0.21	0.18	0.27	-0.08	**-0.05**
CTE.1150.03.240.SAR.BUA001	-0.84	-0.46	-0.65	0.09	0.11	0.60	**-0.10**
CTE.1150.S1.170.SAR.BUA001	-0.69	-0.64	0.70	-0.07	-0.31	0.15	**-0.17**
CTE.1150.02.170.SAR.BUA001	-0.66	-0.92	-0.56	0.26	-0.14	0.39	**-0.22**
CTE.1150.01.120.SAR.BUA001		-0.66	-0.78	-0.38	-0.43	0,00	**-0.42**
CTE.1150.03.140.SAR.BUA001	-1.23	-1.20	-1.04	-0.81	-0.78	-0.51	**-0.89**
CTE.1150.01.060.SAR.BUA001	0.17	-0.56	-1.66	-1.46	-0.70	-1.52	**-0.98**

Fig. 14. Example of average monthly bias of temperature values of different sensors withing a building.

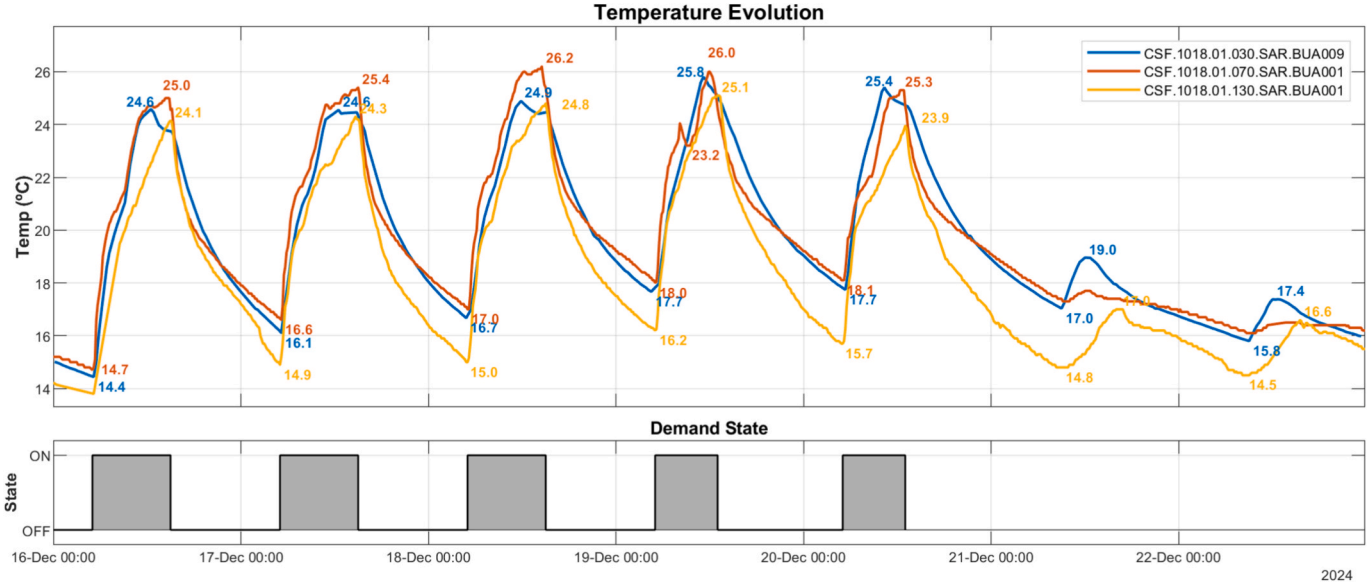

Fig. 15. Temperature evolution and demand state during a week before the implementation of the proposed control system.

methodology and the maximization of its operational effectiveness.

3.3. Methodological Boundaries and Limitations

The applicability of the proposed gradient-based methodology is subject to specific physical boundary conditions and operational constraints. Correct interpretation of the results requires acknowledging the following limitations:

Linearity and Saturation: The linear regression model relies on the system operating within its transient start-up phase. As detailed in Fig. 6, empirical analysis reveals distinct behaviours: in most scenarios, the temperature rise remains linear until the setpoint is approached. Even in instances where the response eventually saturates, the algorithm is designed to isolate the early morning transient window where the response remains linear, effectively discarding the final saturation curve. Consequently, the method's limitation is confined to scenarios where saturation occurs almost immediately at start-up (e.g., during warm transition seasons), leaving insufficient data for a robust linear fit. However, the operational impact of these cases is minimal, as they correspond to periods of low heating demand.

Seasonal and Operational Sensitivity: While the thermal slope is fundamentally a characteristic parameter of each zone, empirical evidence demonstrates its susceptibility to specific boundary conditions, most notably during post-holiday restart periods (e.g., following the Christmas break). In these scenarios, the prolonged absence of heating results in a deep "cold soak" effect where the building's thermal mass cools significantly; upon restart, the structure absorbs a higher fraction of the thermal energy, thereby dampening the rate of air temperature rise ($\Delta T/\Delta t$) compared to the routine winter operation. To a lesser extent, a similar variation is observed during mild transition seasons, where the reduced thermal load may trigger system modulation (partial-load operation), resulting in a lower effective gradient than that

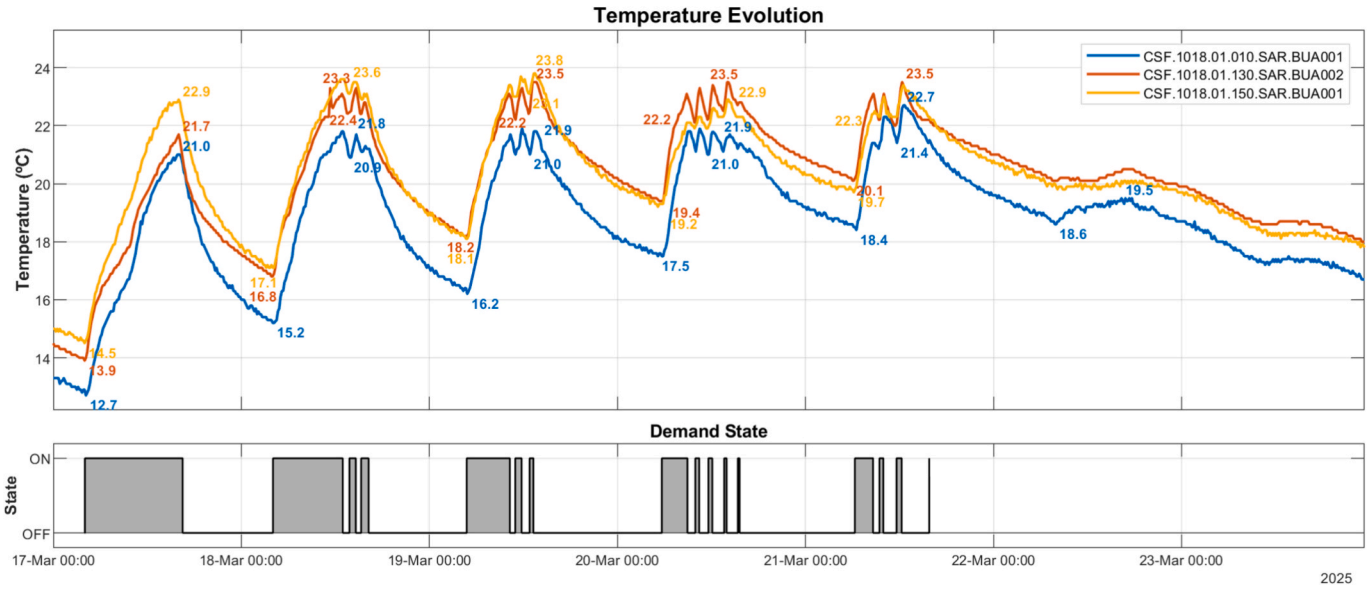

Fig. 16. Temperature evolution and demand state during a week after the implementation of the proposed control system.

Table 6
HVAC startup time (left) and sensor temperature at 8 a.m. (right) before the implementation of the proposed control system.

Day	Startup time	ON time	Sensor	16/12	17/12	18/12	19/12	20/12	Sensor average
16/12/2024	5:00	10.00 h	CSF.1018.01.030.SAR.BUA009	19.87	20.93	21.17	22.43	23.10	21.50
17/12/2024	5:00	10.00 h	CSF.1018.01.070.SAR.BUA001	20.70	21.65	22.00	23.30	21.70	21.87
18/12/2024	5:00	10.00 h	CSF.1018.01.130.SAR.BUA001	19.20	20.10	20.30	21.50	20.90	20.40
19/12/2024	5:00	8.00 h	Date average	19.92	20.89	21.16	22.41	21.90	21.26
20/12/2024	5:00	8.00 h							

Table 7
Percentage distribution of indoor air temperature ranges during occupancy hours before the implementation of the proposed control system.

Day	% t <17ºC	% t 17-20ºC	% t 20-24ºC	% t >24ºC
1	0.00%	5.85%	67.25%	26.32%
2	0.00%	1.61%	61.29%	37.10%
3	0.00%	1.11%	48.89%	49.44%
4	0.00%	0.00%	64.37%	35.06%
5	0.00%	0.00%	72.78%	27.22%

Table 8
HVAC startup time (left) and sensor temperature at 8 a.m. (right) after the implementation of the proposed control system.

Day	Startup time	ON time	Sensor	17/03	18/03	19/03	20/03	21/03	Sensor average
17/03/2025	4:00	12.48 h	CSF.1018.01.010.SAR.BUA001	15.45	18.35	19.00	19.45	19.25	18.30
18/03/2025	4:00	10.67 h	CSF.1018.01.130.SAR.BUA002	16.75	19.95	20.85	21.75	21.45	20.15
19/03/2025	4:50	6.80 h	CSF.1018.01.150.SAR.BUA001	17.55	20.40	20.85	20.85	20.85	20.10
20/03/2025	5:10	4.80 h	Date average	16.58	19.57	20.23	20.68	20.52	19.52
21/03/2025	6:30	3.47 h							

Table 9
Percentage distribution of indoor air temperature ranges during occupancy hours after the implementation of the proposed control system.

Day	% t <17ºC	% t 17-20ºC	% t 20-24ºC	% t >24ºC
1	3.68%	33.13%	63.19%	0.00%
2	0.00%	2.78%	87.96%	9.26%
3	0.00%	0.00%	90.43%	8.95%
4	0.00%	0.00%	99.69%	0.00%
5	0.00%	0.00%	99.04%	0.96%

observed under full-capacity design conditions.

Zoning Resolution and Representative Sensing: In facilities

characterized by low-resolution zoning or the complete absence of zonal control (e.g., single-loop distribution for entire floors), the application of this methodology necessitates a strategic operational compromise. The control logic is constrained to rely on a critical "representative zone" or a spatially weighted average temperature. In scenarios exhibiting high thermal diversity among spaces (e.g., north versus south-facing rooms sharing a common hydraulic circuit), prioritizing the zone with the highest thermal inertia guarantees global comfort compliance but inevitably introduces a penalty of localized overheating in faster-responding areas, in systems lacking local terminal regulation. Consequently, in these instances, the limitation is identified as physical rather than algorithmic. However, this constraint simultaneously represents an opportunity for continuous improvement: the analysis serves to highlight that infrastructure retrofitting, specifically the installation of thermostatic valves or the subdivision of hydraulic circuits, constitutes a prerequisite for achieving effective control optimization.

4. Conclusions

1. This study establishes a methodology for quantifying the thermal response of indoor air to HVAC activation, defined by the temperature rise gradient (°C/h). Application of this method to the heterogeneous building stock at the University of Zaragoza demonstrated significant disparities in thermal performance. The observed monthly average heating gradients varied tenfold, from a low of 0.3 °C/h to a high of 3.0 °C/h. This wide variability underscores that a uniform campus-wide schedule is ill-suited to the unique dynamics of each facility, necessitating a transition to building-specific operational strategies.
2. The thermal response slopes are intrinsically linked to the coupled interplay between the HVAC terminal unit characteristics and the thermal power balance within each zone. While it is a well-established tenet of building physics that air-based systems exhibit faster thermal responses than water-based ones, the effective speed of the system is ultimately determined by the power balance. This balance, defined as the ratio of available HVAC power to thermal demand, is a complex function of the building's physical attributes (e.g., space orientation and enclosures) and the available capacity of the production system. Furthermore, the measured slopes exhibit temporal variation across different days for each sensor location. This variation is primarily influenced by the indoor air temperature at the start-up moment, a variable that implicitly captures the cumulative influence of external weather conditions and the outdoor temperature history.
3. Within this context, this study provides an empirical quantification of these phenomena, establishing a performance hierarchy for the defined terminal HVAC units based on their measured thermal response rates. Systems were ranked from fastest to slowest as follows: Air Handling Units (AHUs) (~1-3 °C/h), floor fan coils (~1-2.5 °C/h), ceiling fan coils (~0.8-1.4 °C/h), conventional radiators (~0.6-1.4 °C/h), underfloor heating (~0.5-0.6 °C/h), and radiant ceilings (~0.5 °C/h). These results empirically corroborate that systems utilizing forced convection (AHUs and fan coils) demonstrate the most rapid capacity to alter space temperatures, whereas systems dominated by high thermal mass (notably underfloor heating) exhibit significant thermal inertia and require earlier activation times.
4. Conventional HVAC scheduling exhibits inherent limitations, as it relies on generalized weather forecasts while failing to account for the unique thermal behaviour of individual buildings, resulting in a suboptimal approach for both energy consumption and occupant comfort. Based on the thermal analysis conducted, a new, dynamic methodology is proposed to optimize HVAC start-up times, transcending static schedules by establishing customized switch-on times for each building or zone. By using the temperature rise gradient (°C/h), it enables the building management system to determine the precise start-up time in real-time by integrating three key data points: the current average indoor temperature from reference sensors, the target indoor temperature (e.g., 19°C for heating mode), and the zone's specific thermal slope. This data-driven approach facilitates the intelligent and coordinated activation of both primary (production) and secondary (distribution) equipment to ensure thermal loads are met precisely at the required time. Adoption of this slope-based, dynamic scheduling model offers the potential for significant improvements in energy efficiency, via the elimination of unnecessary operating time, while simultaneously enhancing occupant thermal comfort. In the pilot implementation, this strategy reduced total HVAC activation time by 16.93% while significantly decreasing the occurrence of overheating during occupancy hours.
5. Beyond operational control, this methodology serves as a powerful diagnostic tool for energy auditing. By characterizing the specific start-up thermal response of each zone of the building, it facilitates the detection of performance gaps, such as system undersizing or unexpected envelope losses, by comparing real-world response rates against theoretical design expectations. This feedback is essential for guiding maintenance, retrofitting decisions, and aligning future HVAC sizing with actual operational dynamics, ensuring that system capacity is tailored to the specific thermal reality of the facility.

In conclusion, the integration of IoT monitoring systems with Spatial Data Infrastructure (SDI) presents a powerful solution for building management. This synergy enables valuable data analysis, while simultaneously allowing for the cost-effective deployment of control systems by eliminating the need for extensive wiring in both new and existing buildings. Ultimately, this data-driven approach offers a viable pathway to enhancing holistic building performance, directly improving energy efficiency, occupant comfort, and the long-term sustainability of the facilities.

CRediT authorship contribution statement

M. García-Monge: Conceptualization, Methodology, Software, Validation, Formal analysis, Investigation, Writing - Original Draft, Writing - Review & Editing, Visualization, Project administration, Funding acquisition. **S. Guillén-Lambea:** Conceptualization, Methodology, Validation, Writing - Review & Editing, Supervision, Project administration, Funding acquisition. **B. Zalba:** Conceptualization, Methodology, Validation, Writing - Review & Editing, Supervision, Project administration, Funding acquisition.

Declaration of competing interest

The authors declare that they have no known competing financial interests or personal relationships that could have appeared to influence the work reported in this paper.

Acknowledgements

The authors would like to express their gratitude to the University of Zaragoza's maintenance service (UZ campus FIDigital initiative, campusfidigital.unizar.es) and UZ Green Office (oficinaverde.unizar.es) for their invaluable contributions to this project.

Funding

Miguel García-Monge Rábanos acknowledges the Government of Aragón for funding this research through the predoctoral contract 24-28 (ORDEN ECU/592/2024, BOA 11/06/2024). Silvia Guillén-Lambea acknowledges the funding from grant RYC2021-034265-I funded by MCIN/AEI/10.13039/501100011033 and "European Union NextGenerationEU/PRTR". With the additional support of the Government of Aragon (Spain) (Reference group T55_20 R).

Data availability

Data will be made available on request.

References

[1] European Commission. Department of Energy., The energy efficiency of buildings, (2020). https://commission.europa.eu/document/download/65660913-cecb-4f2f-b34c-c9bbf9bed1af_es?filename=in_focus_energy_efficiency_in_buildings_es.pdf (accessed April 28, 2024).

[2] The European Parliament and the Council, Directive 2002/91/CE, Relative to the Energy Effcience in Buildings. 2002, (n.d.). https://eur-lex.europa.eu/legal-content/EN/TXT/?uri=celex%3A32002L0091 (accessed May 4, 2024).

[3] UNE-EN ISO 52000-1:2019 Energy performance of buildings - Overarching EPB assessment - Part 1: General framework and procedures (ISO 52000-1:2017), (n.d.). https://www.en.une.org/encuentra-tu-norma/busca-tu-norma/norma?c=N0061777 (accessed November 26, 2025).

[4] B.; Lucas Bonilla, S. Candela, F.; Bustos, G. De Castro, B.M. Pozas, M.L. Bonilla, F. Serrano Candela, P. Bustos, A Methodology for Designing an Automated System to Improve the Thermal Performance of a Large Building in Operation, Buildings 2023, Vol. 13, Page 1938 13 (2023) 1938. https://doi.org/10.3390/BUILDINGS13081938.

[5] Energy performance of buildings - Contribution of building automation, controls and building management - Part 1: General framework and procedures (ISO 52120-1:2021, Corrected version 2022-09), (n.d.). https://www.une.org/encuentra-tu-norma/busca-tu-norma/norma?c=N0070393 (accessed November 8, 2025).

[6] L. Vandenbogaerde, S. Verbeke, A. Audenaert, Optimizing building energy consumption in office buildings: A review of building automation and control systems and factors influencing energy savings, Journal of Building Engineering 76 (2023) 107233, https://doi.org/10.1016/J.JOBE.2023.107233.

[7] A. Gupta, Y. Badr, A. Negahban, R.G. Qiu, Energy-efficient heating control for smart buildings with deep reinforcement learning, Journal of Building Engineering 34 (2021) 101739, https://doi.org/10.1016/J.JOBE.2020.101739.

[8] I. Martínez, B. Zalba, R. Trillo-Lado, T. Blanco, D. Cambra, R. Casas, Internet of Things (IoT) as Sustainable Development Goals (SDG) Enabling Technology towards Smart Readiness Indicators (SRI) for University Buildings, Sustainability 2021, Vol. 13, Page 7647 13 (2021) 7647. https://doi.org/10.3390/SU13147647.

[9] M. García-Monge, B. Zalba, R. Casas, E. Cano, S. Guillén-Lambea, B. López-Mesa, I. Martínez, Is IoT monitoring key to improve building energy efficiency? Case study of a smart campus in Spain, Energy Build 285 (2023) 112882 https://doi.org/10.1016/J.ENBUILD.2023.112882.

[10] W. Li, H. Li, S. Wang, An event-driven multi-agent based distributed optimal control strategy for HVAC systems in IoT-enabled smart buildings, Autom Constr 132 (2021) 103919, https://doi.org/10.1016/J.AUTCON.2021.103919.

[11] T. Zhang, M.P. Wan, B.F. Ng, S. Yang, Model predictive control for building energy reduction and temperature regulation, IEEE Green Technologies Conference (2018-April (2018)) 100–106, https://doi.org/10.1109/GREENTECH.2018.00027.

[12] Directive (EU) 2018/844 of the European Parliament and of the Council of 30 May 2018 amending Directive 2010/31/EU on the energy performance of buildings and Directive 2012/27/EU on energy efficiency., (n.d.). https://eur-lex.europa.eu/eli/dir/2018/844/oj (accessed November 8, 2025).

[13] Smart readiness indicator - European Commission, (n.d.). https://energy.ec.europa.eu/topics/energy-efficiency/energy-efficient-buildings/smart-readiness-indicator_en (accessed May 3, 2024).

[14] P.A. Fokaides, C. Panteli, A. Panayidou, How Are the Smart Readiness Indicators Expected to Affect the Energy Performance of Buildings: First Evidence and Perspectives, Sustainability 2020, Vol. 12, Page 9496 12 (2020) 9496. https://doi.org/10.3390/SU12229496.

[15] L. Pérez-Lombard, J. Ortiz, C. Pout, A review on buildings energy consumption information, Energy Build 40 (2008) 394–398, https://doi.org/10.1016/J.ENBUILD.2007.03.007.

[16] M.M. Islam, S. Shofiullah, Optimizing HVAC Efficiency And Reliability: A Review Of Management Strategies For Commercial And Industrial Buildings, SSRN Electronic Journal (2024), https://doi.org/10.2139/SSRN.5049288.

[17] M. Fadzli Haniff, H. Selamat, R. Yusof, S. Buyamin, F. Sham Ismail, Review of HVAC scheduling techniques for buildings towards energy-efficient and cost-effective operations, Renewable and Sustainable Energy Reviews 27 (2013) 94–103, https://doi.org/10.1016/J.RSER.2013.06.041.

[18] T. Benakopoulos, W. Vergo, M. Tunzi, R. Salenbien, J. Kolarik, S. Svendsen, Energy and cost savings with continuous low temperature heating versus intermittent heating of an office building with district heating, Energy 252 (2022) 124071, https://doi.org/10.1016/J.ENERGY.2022.124071.

[19] M.M. Islam, S. Shofiullah, Optimizing HVAC Efficiency And Reliability: A Review Of Management Strategies For Commercial And Industrial Buildings, SSRN Electronic Journal (2024), https://doi.org/10.2139/SSRN.5049288.

[20] S. Jin, C. Lee, D. Kim, D. Lee, S. Do, Indoor Thermal Environment and Energy Characteristics with Varying Cooling System Capacity and Restart Time, Sustainability 2022, Vol. 14, Page 9392 14 (2022) 9392. https://doi.org/10.3390/SU14159392.

[21] Y. Ruan, J. Ma, H. Meng, F. Qian, T. Xu, J. Yao, Potential quantification and impact factors analysis of energy flexibility in residential buildings with preheating control strategies, Journal of Building Engineering 78 (2023) 107657, https://doi.org/10.1016/J.JOBE.2023.107657.

[22] S. Sun, X. Xing, J. Wang, X. Sun, C. Zhao, Preheating time estimation in intermittent heating with hot-water radiators by considering model uncertainties, Build Environ 226 (2022) 109734, https://doi.org/10.1016/J.BUILDENV.2022.109734.

[23] S. Sun, J. Wang, R. Li, Q. Sun, Estimation of preheating time for building intermittent heating subject to changes in outdoor temperature and solar radiation, Energy Build 317 (2024) 114405, https://doi.org/10.1016/J.ENBUILD.2024.114405.

[24] M. Esrafilian-Najafabadi, F. Haghighat, Occupancy-based HVAC control using deep learning algorithms for estimating online preconditioning time in residential buildings, Energy Build 252 (2021) 111377, https://doi.org/10.1016/J.ENBUILD.2021.111377.

[25] S. Verbeke, A. Audenaert, Thermal inertia in buildings: A review of impacts across climate and building use, Renewable and Sustainable Energy Reviews 82 (2018) 2300–2318, https://doi.org/10.1016/J.RSER.2017.08.083.

[26] Energy Efficiency and Historic Buildings, How to Improve Energy Efficiency, Historic England (2018). https://www.designingbuildings.co.uk/wiki/Thermal_inertia (accessed September 28, 2025).

[27] R. Hu, G. Liu, J. Niu, The Impacts of a Building's Thermal Mass on the Cooling Load of a Radiant System under Various Typical Climates, Energies 2020, Vol. 13, Page 1356 13 (2020) 1356. https://doi.org/10.3390/EN13061356.

[28] K.J. Kontoleon, E.A. Eumorfopoulou, The influence of wall orientation and exterior surface solar absorptivity on time lag and decrement factor in the Greek region, Renew, Energy 33 (2008) 1652–1664, https://doi.org/10.1016/J.RENENE.2007.09.008.

[29] F. Karlsson, P. Fahlén, Impact of design and thermal inertia on the energy saving potential of capacity controlled heat pump heating systems, International Journal of Refrigeration 31 (2008) 1094–1103, https://doi.org/10.1016/J.IJREFRIG.2007.12.002.

[30] M. Fan, H. Cheng, M. Nian, S. Xie, Performance Study of Intermittent Heating Mode Combining Air-Source Heat Pump with Radiator in Hot Summer and Cold Winter Zones of China, Advances in Civil Engineering 2024 (2024) 1661363, https://doi.org/10.1155/2024/1661363.

[31] K.A. Antonopoulos, E.P. Koronaki, On the dynamic thermal behaviour of indoor spaces, Appl Therm Eng 21 (2001) 929–940, https://doi.org/10.1016/S1359-4311(00)00091-0.

[32] G.M. Soret, P. Vacca, J. Tignard, J.P. Hidalgo, C. Maluk, M. Aitchison, J.L. Torero, Thermal inertia as an integrative parameter for building performance, Journal of Building Engineering 33 (2021) 101623, https://doi.org/10.1016/J.JOBE.2020.101623.

[33] J.A. Orosa, A.C. Oliveira, A field study on building inertia and its effects on indoor thermal environment, Renew, Energy 37 (2012) 89–96, https://doi.org/10.1016/J.RENENE.2011.06.009.

[34] M. Herrando, D. Cambra, M. Navarro, L. de la Cruz, G. Millán, I. Zabalza, Energy Performance Certification of Faculty Buildings in Spain: The gap between estimated and real energy consumption, Energy Convers Manag 125 (2016) 141–153, https://doi.org/10.1016/J.ENCONMAN.2016.04.037.

[35] I. Uriarte, A. Erkoreka, A. Legorburu, K. Martin-Escudero, C. Giraldo-Soto, M. Odriozola-Maritorena, Decoupling the heat loss coefficient of an in-use office building into its transmission and infiltration heat loss coefficients, Journal of Building Engineering 43 (2021) 102591, https://doi.org/10.1016/J.JOBE.2021.102591.

[36] Q. Gao, M. Demoulin, H. Wang, S. Riaz, P. Mancarella, Flexibility Characterisation from Thermal Inertia of Buildings at City Level: A Bottom-up Approach, UPEC 2020 - 2020 55th International Universities Power Engineering Conference, Proceedings (2020). https://doi.org/10.1109/UPEC49904.2020.9209795.

[37] S. Huang, S. Katipamula, R. Lutes, Experimental investigation on thermal inertia characterization of commercial buildings for demand response, Energy Build 252 (2021) 111384, https://doi.org/10.1016/J.ENBUILD.2021.111384.

[38] S.Ø. Jensen, A. Marszal-Pomianowska, R. Lollini, W. Pasut, A. Knotzer, P. Engelmann, A. Stafford, G. Reynders, IEA EBC Annex 67 Energy Flexible Buildings, Energy Build 155 (2017) 25–34, https://doi.org/10.1016/J.ENBUILD.2017.08.044.

[39] LoRa Alliance, LoRaWAN Specification, (n.d.). https://lora-alliance.org/about-lorawan/ (accessed October 15, 2025).